



Norwegian University of  
Science and Technology

# Investigation of some compounds and gold nanoparticles for photodynamic therapy

**Tom André Hansen**

Master of Science

Submission date: June 2018

Supervisor: Mikael Lindgren, IFY

Co-supervisor: Odrun Gederaas, IFY

Norwegian University of Science and Technology  
Department of Physics



## Abstract

In this thesis several chemical compounds for possible use as photosensitizers (PS) in photodynamic therapy (PDT) have been investigated. First a photophysical characterization was performed using different spectroscopic techniques. With these methods the absorption, fluorescence, fluorescence lifetime and quantum yield, triplet excited state absorption and singlet oxygen luminescence, were quantified. Furthermore, experiments using cancer cell models were carried out to investigate possible compounds for PDT. The compounds which have been characterized can be divided into two groups; three different protoporphyrins and three dye compounds, all known to produce singlet oxygen. Among the protoporphyrins, Protoporphyrin A showed higher absorption, fluorescence and singlet oxygen production and lifetime compared to Protoporphyrin B and Protoporphyrin IX. Comparing the three singlet oxygen producing compounds, both eosin B and perinaphthenone showed very weak fluorescence, while erythrosin B had a much stronger fluorescence. Perinaphthenone yielded a better singlet oxygen production and longer singlet oxygen lifetime while eosin B showed no singlet oxygen luminescence.

The cell lines AY27 (cancer from rat bladder) and WiDr (cancer from human colon) were used in PDT experiments. The WiDr cells were used in photobleaching experiments containing cells treated with Protoporphyrin A or Protoporphyrin B. The exposure time of blue light (412 nm) ranged from no light up to 600 seconds. An investigation of the addition of gold nanoparticles to erythrosin B, in order to enhance the effect of PDT, was performed after initial photophysical characterization. The toxicity of gold nanoparticles were determined by checking the cell viability with the use of a MTT-assay. The results from this assay were studied to obtain a concentration of gold nanoparticles which were added to erythrosin B in combination by light treatment (532 nm) of AY27 cells. This yielded no significant difference between cells treated with an addition of gold nanoparticles, as opposed to those without.



## Sammendrag

I denne masteroppgaven har flere kjemiske forbindelser blitt undersøkt for mulig anvendelse som fotosensibiliserende stoff i fotodynamisk terapi (PDT). Først ble en fotofysisk karakterisering utført ved hjelp av forskjellige spektroskopiske teknikker. Disse metodene ble brukt til å kvantifisere absorpsjonen, fluorescens, fluorescenslevetid og kvanteutbytte, triplet eksitert tilstand-absorpsjon og singlett oksygen luminescens. Videre ble eksperimenter som brukte kreftcellemodeller utført for å undersøke mulige forbindelser som kan anvendes i PDT.

Forbindelsene som har blitt karakterisert kan deles inn i to grupper; tre forskjellige protoporfyriner og tre fargestoffforbindelser, som alle er kjent for å produsere singlett oksygen. Blant protoporfyrinene, viste Protoporphyrin A sterkere absorpsjon, fluorescens og singlett oksygen-produksjon og -levetid sammenlignet med Protoporphyrin B and Protoporphyrin IX. En sammenligning av de tre singlett oksygen-produserende forbindelsene viste at eosin B og perinaphthenone hadde veldig svak fluorescens, mens erythrosin B hadde mye sterkere fluorescens. Perinaphthenone ga en bedre singlett oksygenproduksjon og lengre singlett oksygenlevetid, samtidig som eosin B ikke viste noen tegn til singlett oksygen luminescens.

Cellelinjene AY27 (kreft fra rotteblære) og WiDR (kreft fra menneskelig tykktarm) ble brukt i PDT-eksperimenter. WiDr-cellene ble brukt i fotoblekingseksperimenter med celler som hadde blitt behandlet med enten Protoporphyrin A eller Protoporphyrin B. En undersøkelse av gullnanopartikler tilsatt til en PS, for å forsterke effekten av PDT, ble gjennomført etter fotofysisk karakterisering. Toksisiteten til gullnanopartiklene ble bestemt ved sjekke celleviabiliteten ved bruk av en MTT-analyse. Resultatene fra denne analysen ble studert for å finne en konsentrasjon av gullnanopartikler som ble tilsatt erythrosin B i kombinasjon med lysbehandling (532 nm) av AY27-celler. Dette resulterte i ingen signifikant forskjell mellom celler behandlet med en tilsetning av gullnanopartikler, i motsetning til de uten.



## Preface

This thesis is the final step of my education here at NTNU. It has been a long and tough education, but I have learned a lot about courses and myself throughout these years. First and foremost will I thank my supervisor Prof. Mikael Lindgren (Department of Physics, NTNU) and co-supervisor Odrun A. Gederaas (Department of Chemistry, NTNU). The ideas, suggestions, experience and overall helpful discussions have been essential to the completion of this thesis. The patience and understanding you have shown is very much appreciated.

I would also like to thank PhD student Andreia Granja for all the help and collaboration helping the improvement of this thesis and PhD student Per Magnus Walmsness for the guidance and assistance with the experimental work.

Thank you Thor Bernt Melø for always having the time to help or give advice, on experiments and theory alike, and to Kristin G. Sæterbø for the training in the cell lab. Without support of Erling Hannaas, Roland Richter and Sigurd A. Borstad this last year things would have been a lot more difficult, thank you very much.

Finally I would like to thank Audun Tamnes and Ingeborg G. Hem for the support throughout this time in Trondheim, you two made grey days much brighter.



# Contents

Abstract . . . . .	iii
Sammendrag . . . . .	v
Preface . . . . .	vii
<b>1 Introduction</b>	<b>1</b>
1.1 History . . . . .	1
1.2 Photodynamic therapy . . . . .	2
1.3 The content and purpose of the study . . . . .	5
<b>2 Light interacting with matter</b>	<b>7</b>
2.1 Absorption of light . . . . .	7
2.2 Emission of light . . . . .	9
2.3 Radiationless de-excitation processes . . . . .	12
2.4 Quantum efficiency . . . . .	12
2.5 Excited state lifetime . . . . .	13
2.6 Excited state absorption . . . . .	14
2.7 Photobleaching as indication of photodynamic therapy . .	14
2.8 Cell survival study- MTT assay . . . . .	15
<b>3 Materials and methods</b>	<b>17</b>
3.1 Absorption spectroscopy . . . . .	17
3.2 Emission spectroscopy . . . . .	18
3.3 Measure of quantum yield . . . . .	20
3.4 Fluorescence lifetime- time-correlated single-photon counting . . . . .	20

3.5	Excited state absorption spectroscopy . . . . .	22
3.6	Singlet oxygen luminescence . . . . .	23
3.7	Cultivation of cancer cells . . . . .	25
3.8	Cell survival assay (MTT) . . . . .	26
3.9	Photobleaching experiment . . . . .	27
3.10	Photodynamic treatment of erythrosin B and gold nanoparticles . . . . .	27
3.11	Preparation of samples . . . . .	28
3.12	Estimation of errors . . . . .	29
<b>4</b>	<b>Results</b>	<b>33</b>
4.1	Photophysical properties of tested PS . . . . .	33
4.2	Viability & PDT results . . . . .	43
<b>5</b>	<b>Discussion</b>	<b>55</b>
5.1	Evaluation of the protoporphyrins . . . . .	55
5.2	The influence of gold nanoparticles in PDT . . . . .	58
5.3	Evaluation of singlet oxygen yielding compounds . . . . .	59
5.4	Future work . . . . .	61
<b>6</b>	<b>Conclusion</b>	<b>63</b>
	<b>Bibliography</b>	<b>65</b>
<b>A</b>	<b>Additional plots and results</b>	<b>73</b>
A.1	Triplet state decay . . . . .	73
A.2	Singlet Oxygen . . . . .	73
<b>B</b>	<b>PCI Biotech LumiSource</b>	<b>81</b>
<b>C</b>	<b>Structural information</b>	<b>85</b>

# Chapter 1

## Introduction

### 1.1 History

The use of a light therapeutically goes all the way back to ancient Egypt with the Egyptians seeing a connection between the sun and health. The use of sunbaths as a way to improve the health is much more documented by the Greeks and the Romans [1]. The first renowned use of light in medicine came with Niels Rydberg Finsen which used it to treat smallpox and then later tuberculosis of the skin (*Lupus vulgaris*), which the latter earned him the Nobel prize in 1903 [2, 3]. The first reports of dyes which are nontoxic by themselves could kill cells with light were made by Oscar Raab, a medical student working with Professor Hermann Von Tappeiner in Munich around 1899 [4]. Later in 1904 Von Tappeiner and Albert Jodlbauer demonstrated that the presence of oxygen was a central part of what they in 1907 called "photodynamic action" [5]. The introduction of porphyrins as dye which causes photosensitization was discovered when the German Friedrich Meyer-Betz gave himself an injection of 200 mg of hematoporphyrin (HP) in 1913. This was in order to see if the phototoxic results that had been previously seen in mice also could occur in humans [6]. Meyer-Betz confirmed the phototoxicity in humans at the expense of swelling and pain in the areas that were exposed to sun light. The use of HP would play an important role in the development of what

would be known as photodynamic therapy with the discovery by Policard of the HP's characteristic red fluorescence from malignant tumors in a laboratory rat in 1924 [7]. This would mark the beginning of the important role porphyrins in PDT, with the first observation of red porphyrin fluorescence in tumors first observed by Policard which was further supported by Auler and Banzer in 1942 and then later by Figge and Weiland in 1948 [8]. It turned out that HP was so impure that the fluorescence was due to a mixture of porphyrins, so Samuel Schwartz purified into what he called hematoporphyrin derivatives (HpD), which Lipson extensively studied the localizing properties of in the 1960s [9]. Both Lipson and Thomas Dougherty would report photodynamic therapy in breast cancer and in tumors in rats and mice, during the 1970s [10]. Today photodynamic therapy has reached the point of clinical treatment of solid malignant and/or flat tumors and have been approved in several countries, among these are USA, Japan and Russia. [11].

## 1.2 Photodynamic therapy

Photodynamic therapy (PDT) consists of three central parts: a photosensitizer (PS), light and oxygen. The main advantages of this treatment are the low number of side effects compared to chemotherapy and that PDT is less invasive than surgery [12].

The PS is introduced into the body, carried by the blood to the area where the cancer is situated and then exposed to light. This catalyzes a reaction, where the PS reacts with the oxygen in the cell tissue or the environment. The reaction can either create reactive oxygen species, through an electron transfer or create singlet oxygen, through an energy transfer via a triplet excited state. These processes are known as a type I or type II reactions, respectively. Both the reactive oxygen species and the singlet oxygen can destroy the cancer cells. The research is focusing on improving the efficiency of the photosensitizers. High tumor and cancer cell selectivity, while having low dark toxicity (cell death caused by the PS

without the illumination) are desired properties.

In order to evaluate these properties spectroscopic characterization is necessary. The absorption spectrum will show if there is sufficient absorption for wavelengths suited for the actual treatment. In addition a higher absorption will result in fewer PS-molecules required for the treatment. The wavelengths for which the PS absorbs must also have the ability to penetrate the skin. The emission spectrum will provide information about the transition from the first excited state to ground state, first of all if the transition exists. With this information one can then further investigate the lifetime of fluorescence, and determine if it enables the possibility of a inter-system crossing (ISC) into a triplet state. Oxygen is one of the few molecules with a triplet ground state and is always present in our bodies. This triplet ground state can then react with the PS in the first excited triplet state and generate singlet oxygen or other reactive oxygen species (ROS) [13]. The amount of oxygen is limited in the cells due to consumption of it, for example by the mitochondria inside cells or the PDT mechanism itself.

### 1.2.1 The photosensitizers

The PS is one of the key elements in PDT and in the beginning of clinical treatment the PS used were HpD and Photofrin<sup>®</sup>. The research is continuously aiming for an increasingly efficient PS [14]. The properties of an ideal PS are [15]:

- Efficient singlet oxygen production.
- High absorption coefficient in the region of 700-800 nm.
- No dark toxicity (no light), minimal to no skin photosensitivity and selective accumulation in tumors.
- Chemical structure which can easily distribute in the body. That means; easily uptake in cells by the crossing of cell membranes.

- A high tumor selectivity and rapid clearance from body after treatment.
- A chemically pure compound with high yielding or short synthesis.

A type of photosensitizer which have been studied thoroughly are porphyrins. The general structure of a porphyrin is a tetrapyrrole ringlike structure. A derivative of porphyrin known as protoporphyrin is naturally occurring in our bodies as a natural precursor to hemes e.g. hemoglobin [16]. An illustration of the heme pathway is shown in figure 1.1 [17]. The structure for protoporphyrin IX (PpIX), which is a porphyrin derivative, is shown in figure 1.2,[18]. If 5-aminolevulinic acid is added outside the cancer cells then a endogenous production of PpIX will be catalyzed, causing tumors to accumulate a large concentration of PpIX. This is foundation of what is known as ALA-PDT [19].

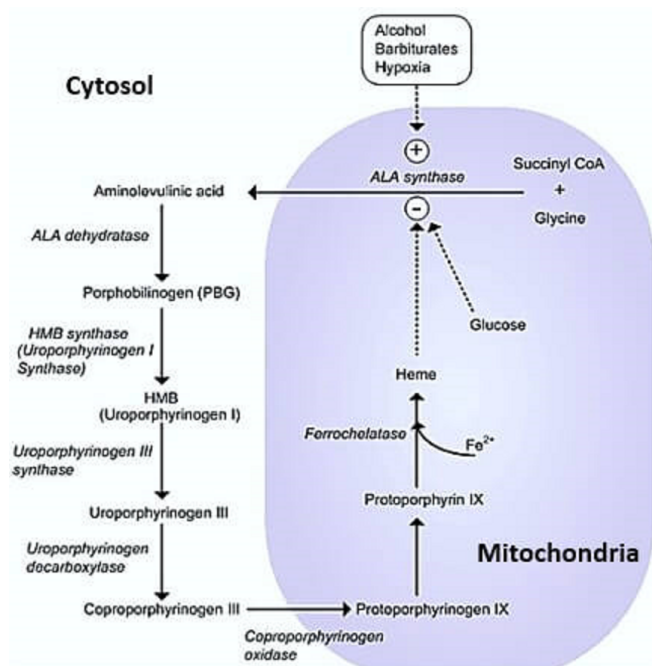


Figure 1.1: Overview over the different steps in the heme synthesis [17].

However, there many classes of molecular systems that can be used to form a relatively stable excited triplet state. Stable enough to allow

diffusion until it meets a dioxygen molecule, and hereby change its triplet state to a singlet state dioxygen. These are also potential PS that can be used in PDT.

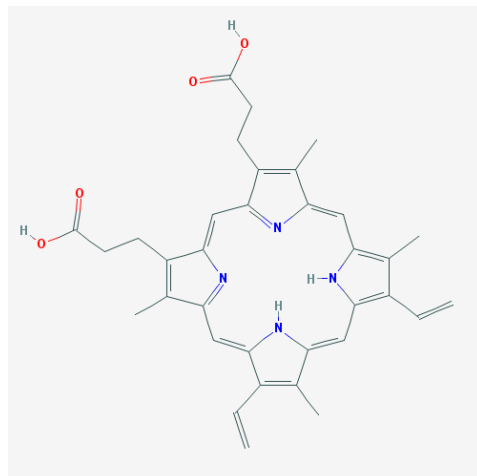


Figure 1.2: Structural formula of protoporphyrin IX. The ringlike structure which includes four nitrogen atoms is known as a tetrapyrrole [18].

### 1.3 The content and purpose of the study

The experiments in this thesis are all aimed to characterize compounds to be used as possible PS in PDT. The compounds can be divided into two types: protoporphyrins and known singlet oxygen producers. The protoporphyrins is a collaboration with "Universite d'Avignon et des pays de Vaucluse" in Paris, France, which has synthesized molecules with intent of future use for PDT. These protoporphyrins molecules were modified to have improved solubility however, their structures are not disclosed here as they are included in a patent application.

The known singlet oxygen producers are eosin B, erythrosin B and perinaphtenone. In collaboration with PhD student Andreia Granja from the University of Porto in Porto, Portugal, the effects of gold nanoparticles added to erythrosin B, were studied.

The basic photophysical properties that were measured were absorption, fluorescence, quantum yield and fluorescence lifetime. In addition the excited state absorption, triplet state decay and the singlet oxygen luminescence were also investigated. The photobleaching effects of the protoporphyrins were investigated as an extension of experiments from the previous semester. The PDT effect of erythrosin B with and without gold nanoparticles was checked using MTT-assays of different concentrations and light treatment.

# Chapter 2

## Light interacting with matter

### 2.1 Absorption of light

Atoms and molecules all have electrons with a certain set of discrete energies. The properties of the atoms or molecules are governed by this set. This is further dependent on which type of atoms is present, the structure of the molecules and the total number of electrons in the system. When the system is not affected by any external interactions which can increase or decrease the system's energy, the total energy of the electrons will be as low as possible [20]. This electronic energy level is known as the system's ground state.

The next electronic state of higher energy is known as the first excited state, the next state is known as the second excited state and so on. The electrons (and thus the whole molecule) can through an external interaction, obtain more energy and depending on the amount of energy, jump to one of these excited energy states for a short period of time. One example of such an external interaction is the absorption of a photon [20].

It is experimentally possible to measure how much energy the molecule is absorbing by measuring the incident intensity,  $I_0$ , and the transmitted intensity,  $I$ , through a sample of the molecule of interest, at different wavelengths. Assume you have a monochromatic light beam passing through a thin slice  $dx$  with  $N$  molecules for each increment until the to-

tal path length  $L$  of the sample is reached.

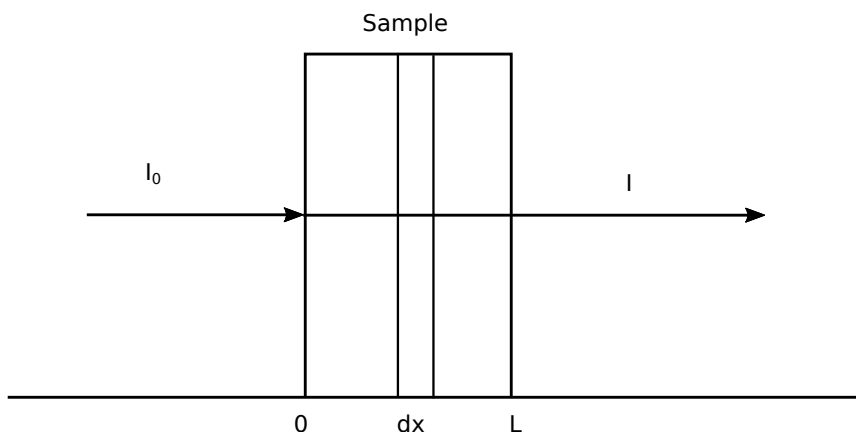


Figure 2.1: Absorption of light passing through a sample.

The relative intensity  $dI'/I'$  corresponds to the absorption of the molecules. The Beer-Lambert law then says that

$$Ndx = -\frac{1}{\sigma} \frac{dI}{I} \quad (2.1)$$

$\sigma$  is the absorption cross-section and the fraction  $-\frac{1}{\sigma}$  is the constant of proportionality between the increment of absorbing molecules and the light which is absorbed [21]. By integrating both sides:

$$\int_{I_0}^I \frac{dI}{I} = -\sigma N \int_0^L dx. \quad (2.2)$$

This gives the definition of the absorbance, or rather the optical density  $A(\lambda)$ , of the sample as

$$\log\left(\frac{I_0(\lambda)}{I(\lambda)}\right) = A(\lambda) = (-\log e) \ln\left(\frac{I_0(\lambda)}{I(\lambda)}\right) = \sigma N l \log e. \quad (2.3)$$

It is more common to use the concentration  $C$  in liter per mole rather than  $N$  which can be obtained from  $N = N_{AV}C/10^3$   $N_{AV}$  is Avogadro's

number<sup>1</sup>. Inserting this yields the final form of the Beer-Lambert law

$$A(\lambda) = \epsilon(\lambda)CL. \quad (2.4)$$

$\epsilon(\lambda) = \sigma N_{Av} 10^{-3} \log e$  is known as the extinction coefficient and is a molecular property with units  $\text{mol}^{-1} \text{cm}^{-1}$ . This provides with an experimental relationship between absorption, the extinction coefficient and concentration.

## 2.2 Emission of light

Excited atoms and molecules also have the ability of emitting a photon. If a electron is already in an excited state it can jump to a lower energy state, either by interaction with incoming radiation or spontaneously by itself, emitting a photon in the process. The former process is called stimulated emission and the latter is known as spontaneous emission. Emission of light is a reaction to an input energy and is generally known as luminescence. The special case where the input energy is gained from radiation is known as photo-luminescence. Photo-luminescence can further be divided into to fluorescence and phosphorescence. This division comes from the electrons and their intrinsic angular momentum known as spin [22].

The electron can either have spin up or spin down. Tied to the spin property is the Pauli exclusion principle, which states that paired electrons, electrons sharing the same molecular orbital, must have different spin [23]. This gives rise to different energy levels when the system is excited. In the ground state if one electron have spin up and the other have spin down, the system is said to be in a singlet state. By exciting one of the electrons without changing their spin, the system is in a excited singlet state. If one of the paired electrons is excited to another state, then they no longer are in the same orbital and are no longer bound by the

---

<sup>1</sup> Avogadro's number  $N_{Av} = 6.022 \times 10^{23} \text{mol}^{-1}$

Pauli exclusion principle.

It is then possible for the excited electron to change its spin in a process called inter-system crossing (ISC) [24]. This system with a pair of electrons having parallel spin is known as a triplet state. The inter-system conversion from a singlet vibrational state to a triplet vibrational state is isoenergetic, but after vibrational relaxation the electron has a slightly lower energy than the corresponding singlet state. Depending on if the emission of a photon originates from the singlet state or the triplet state it is called fluorescence or phosphorescence.

### 2.2.1 Fluorescence

After absorbing energy from incoming radiation the excited molecule can relax to its ground state by the emission of a photon. The most common time scale of this process is around  $10^{-10}$  to  $10^{-8}$  seconds and is known as fluorescence. Molecules with the ability to fluoresce are called fluorophores. The photon energy of the fluorescent light is often less than the energy of the photon that was absorbed. This is due to the different vibrational structure of the electronic energy levels. The transition from a higher vibrational for example the  $\nu'' = 2$  state, to a lower vibrational state  $\nu'' = 0$  is called vibrational relaxation. The vibrational relaxation is radiationless and happens on a timescale much faster than the fluorescence [25].

The energy level from which the molecule is fluorescing is therefore lower. Any excitation of the electron to excited states higher than the first excited state will relax from that state isoenergetic through a non-radiative process called internal conversion. The different energy levels and transitions have been intuitively visualized by presenting them in what is called a Jablonski diagram (see figure 2.2) [26].

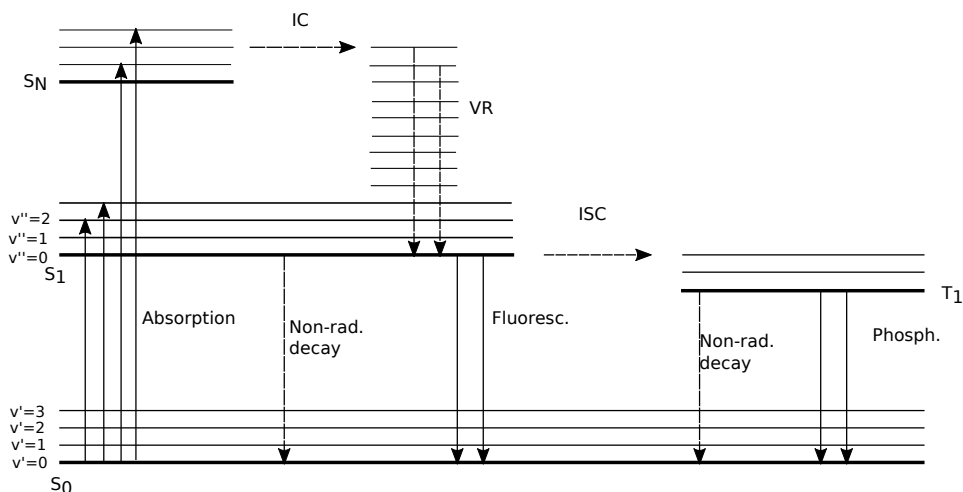


Figure 2.2: The Jablonski diagram providing a visual representation of the transitions between different electronic and vibrational states. S and T denotes the singlet state and triplet state, respectively.

### 2.2.2 Quenching

The many different processes which results in the decrease of the intensity of the fluorescence are known as quenching. Among these one of the most common is collisional quenching. The excited fluorophore then collides with a different molecule, called a quencher, in the solution causing the deexcitation of the fluorophore. This collision is due to the diffusion in the sample solution. Other quenching mechanisms are that the quenchers form non-fluorescent complexes with the fluorophore or simply that the quencher attenuates the incident light reaching the fluorophore. Examples of molecules that can act as quenchers are oxygen, halogens and amines [25].

### 2.2.3 Photobleaching

Any photochemical reaction between light and a fluorophore resulting in that the fluorophore is loosing its ability to fluoresce, is known as photobleaching. This is usually caused by changes in the chemical structure of the fluorophore. One can distinguish two types of irreversible pho-

photobleaching known as photomodification and true photobleaching. The former one refers to a loss of fluorescence for some wavelengths, while the latter refers to a total loss of fluorescence [27].

### 2.2.4 Phosphorescence

Emission of a photon from the triplet state is also possible and is known as phosphorescence. This is a much slower process than fluorescence with lifetimes in the range of  $10^{-6}$  to  $10^{-3}$  seconds, typical for molecules in solvent phase. Because of this long lifetime, the majority of the excited molecules are more likely to relax to the ground state through other processes. Thus, in most cases the phosphorescence is much weaker than the fluorescence. Both the long lifetime and weaker phosphorescence, are due to the low possibility of a transition from the triplet states to the ground singlet state or the other way around, respectively. The process going from the singlet state to the triplet state or vice versa by absorbing or emitting a photon is spin-forbidden.

## 2.3 Radiationless de-excitation processes

As shown in figure 2.2, there are in addition to vibrational relaxation other ways of deexcitation of the molecule without emission of photons. Internal conversion (IC) is one and refers to the redistribution of energy when the molecule transitions to the first excited state from an excited state higher state than the first excited state. The molecule can as well relax to the ground state through non-radiating process either colliding with other molecules or radiating heat similar to IC.

## 2.4 Quantum efficiency

The quantum efficiency (QE) or quantum yield (QY) of a molecule says something about how many photons the molecule emits compared to

the photons absorbed. The quantum efficiency of fluorescence is denoted as  $\Phi$  yielding the expression

$$\Phi_F = \frac{\text{number of emitted fluorescence photons}}{\text{number of absorbed photons}} \quad (2.5)$$

If the molecule emits one photon for each photon it has a QE of 1.0, being the highest achievable value. This rarely occurs, due to the possibility of radiationless deexcitation as mentioned in the previous section and other processes which reduces the fluorescence. An equation for the QE which takes into account these processes is written as:

$$\Phi_F = \frac{\kappa_F}{\kappa_F + \kappa_{NF}}. \quad (2.6)$$

Where  $\kappa_F$  is the probability of the fluorescence and  $\kappa_{NF}$  is the probability of non-fluorescent processes. The inverse of these two values can be used to find the lifetime of the excited state of the molecule.

## 2.5 Excited state lifetime

Up to now, we have seen that there are several ways for an excited molecule to relax back to the ground state. An important molecular property is the radiative decay time, how long it takes before the molecule is deexcited due to radiative processes like fluorescence. The excited state lifetime is the average time the molecule spends in the excited state before returning to the ground state. Assume we have a sample of fluorophores irradiated with light which yields an initial population  $n_0$  in the excited. The number of fluorophores in the excited state at time  $t$ ,  $n(t)$ , decays with a rate (given from the previous section)  $\kappa_F + \kappa_{NF}$  given by

$$\frac{dn(t)}{dt} = -(\kappa_F + \kappa_{NF})n(t). \quad (2.7)$$

We usually measure the fluorescence in intensity and  $n(t)$  being proportional to the intensity, an integration of 2.7 yields the expression for

the single exponential decay

$$I(t) = I_0 \exp^{-t/\tau}, \quad (2.8)$$

where  $I_0$  is the intensity at time zero and  $\tau$  is the decay. Comparing 2.7 and 2.8 we see that  $\tau = \frac{1}{\kappa_F + \kappa_{NF}}$ . The lifetime is the inverse of the sum of the processes that causes the depopulation of the excited state.

## 2.6 Excited state absorption

Previously it was mentioned that the molecule could absorb a photon with an energy equal to or larger than the gap between two energy levels of the molecule. If we irradiate a sample with a strong enough intensity and the lifetime of the excited state is sufficiently long the sample have the possibility of its electrons in the excited state, absorbing another photon to be excited further to an even higher energetic state. As triplet states are long-lived so called excited state absorption (ESA) is a useful technique to study triplet presence and kinetics.

## 2.7 Photobleaching as indication of photodynamic therapy

The porphyrins-compounds which are possible photosensitizers are light sensitive and have the ability to fluoresce. This can be used to record at the fluorescence spectrum of cells treated with photosensitizer and given different light doses. A light dose is defined as the irradiance multiplied with the time the cells have been exposed to the light and is usually measured in  $\text{J}/\text{cm}^2$ . It can be calculated from the effect of the light source, the area of sample containing the cell and the exposure time. For a majority of the photobleaching of PS with oxygen present are chemical processes containing singlet oxygen and or reactive oxygen species (ROS). The degree of photobleaching can the be used to give an indication to

the efficiency of the photosensitizer, but have to be confirmed with complementary cell viability measurements [28].

## **2.8 Cell survival study- MTT assay**

In order to assess the cytotoxicity of the photosensitizers it is necessary to detect the percentage of living cells after treatment. The use of tetrazolium salts and particularly 3-(4,5-imethylthiazol-2-yl)-2,5-diphenyltetrazolium bromide, otherwise known as MTT have proven to be a reliable and fast method to estimate the number of living cells. This colometric method utilizes that the yellow and water soluble compound 3-(4,5-dimethylthiazol-2-yl)-

2,5-diphenyltetrazolium bromide is reduced to formazan or more specifically 1-(4,5-dimethylthiazol-2-yl)-3,5-diphenylformazan. The latter is both purple and water insoluble. This reduction is a result of living cells with a functional mitochondrial hydrogenase. The purple formazan can be dissolved in acidified isopropanol as first described by Mosman [29]. Then absorption spectroscopy can be used to estimate the number of living cells when compared to a reference sample.



# Chapter 3

## Materials and methods

The interaction of light with matter is a frequently and naturally occurring phenomenon. Irradiating atoms and molecules with electromagnetic radiation such as light, as a function of frequency or wavelength and study the resulting reaction is a method known as spectroscopy [30]. Spectroscopy can be used to determine structural and dynamical properties of atoms and molecules.

### 3.1 Absorption spectroscopy

Optical absorption is found by measuring both the incoming and outgoing light from the sample and varying the wavelength of the radiation source. A typical setup is shown in figure 3.1. The resultant spectrum is either a plot of the extinction coefficient,  $\epsilon$ , or the absorbance  $A$ , as a function of wavelength (often in nano-meters). The information gathered from  $\epsilon(\lambda)$  is used to characterize the molecular absorption. The most common is determining the wavelength where the absorption is largest  $\lambda_{max}$ , and the corresponding value of  $\epsilon(\lambda_{max})$ .

Experimentally, the molecules were usually dissolved in an organic or inorganic solvent in special cuvettes produced specially for spectroscopy. The solvents have low absorption in the wavelength region of interest. The results are obtained using a detector, which measures the transmit-

ted intensity from the sample. All measurements however will also contain contributions from the solvent and the cuvette. In order to only get the absorption from the sample some preparations are necessary. This is done by also making a reference sample only containing the cuvette and the solvent.

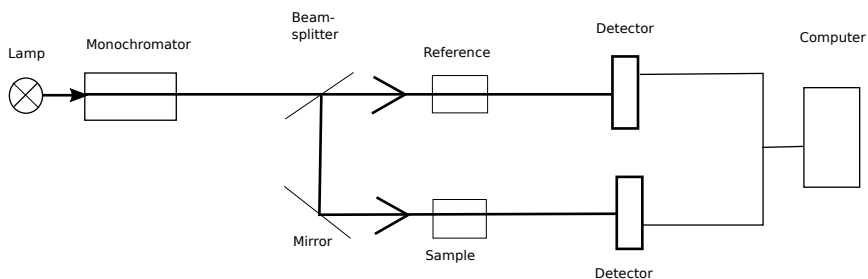


Figure 3.1: A schematic description of an absorption spectrometer

By using a beamsplitter both the sample and the reference can be irradiated simultaneously and the reference containing the contribution from both the cuvette and the solvent can be subtracted from the total absorption, this is known as the baseline.

One should try to keep the value of the absorbance below 1.0 optical density (O. D.) as equation (2.4) is only valid for sufficiently small values of the absorbance. If the values are larger than 1.0 the measurements could be inaccurate because of non-linear effects. All the absorption measurements were done using a Hitachi U-3010 spectrophotometer with the software UV-Solutions (Tokyo, Japan).

## 3.2 Emission spectroscopy

In order to measure the fluorescence emission spectrum, one excites the sample at specific wavelength and varies the position of a grating, giving a scan of wavelengths the detector is measuring. A schematic is shown in figure 3.2. The direction of the light which is measured is usually at a right angle compared to the light exciting the sample in order to minimize background signals and scatter from the excitation light.

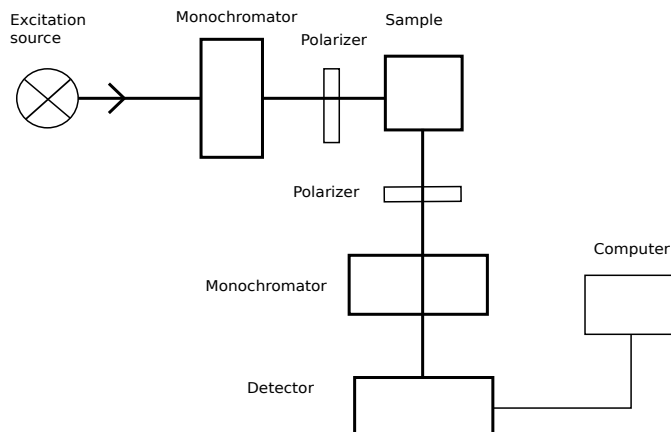


Figure 3.2: A schematic of an emission spectrometer

The choice of excitation wavelength can be retrieved experimentally from the absorption spectrum. The emission spectrum gives information about which wavelengths the sample fluoresce and the strength of the fluorescence of each wavelength. The position of the maximum fluorescence is sensitive to the environment and in particular the solvent.

As pointed out in section 2.2.1 the photon energy of the fluorescence is lower than the energy of the absorbed light. This is due to the solvent where polar groups relax their position in response to the excited molecule before emission. This will lower the energy of the excited state and gives a shift between the absorption and emission. The difference between the wavelength of maximum absorption and emission is known as the Stokes's shift. The energy aspect will be further elaborated in the results and discussion section.

When measuring the fluorescence a sample of just the solvent was also measured and subtracted from the spectra using the software. The values obtained were the ones which were emission corrected by the software. The fluorescence spectra and the integrated fluorescence for quantum yield were obtained using the Horiba PTI Fluorescence Master with the software FelixGX Data Analysis.

### 3.3 Measure of quantum yield

In order to find the quantum yield one uses both the absorption and fluorescence signal of several concentrations. This requires great care when doing the measurements as especially absorbance measurements are sensitive to errors at low concentrations. The most common way is to determine the relative quantum yield for the molecule and compare the results with a known reference sample under identical experimental conditions. By taking the integrated fluorescence for a given excitation wavelength, and plot it as a function of absorbance one gets a set of data points. Using linear regression on those points and taking the gradient of that line will yield the relative quantum yield. The mathematical relation is given by

$$\Phi_S = \Phi_{Ref} \frac{A_{Ref} F_S n_S^2}{A_S F_{Ref} n_{Ref}^2}. \quad (3.1)$$

The "S" and the "Ref" indicates the sample and the reference, respectively. A is the absorbance, F is the fluorescence and n is the refractive index of the solvent. It is assumed that the reference and the sample are excited at the same wavelength. The value of the absorption should be kept below 0.1 OD to avoid self-absorption and inner filter effects [20].

### 3.4 Fluorescence lifetime- time-correlated single-photon counting

Time-correlated single-photon counting (TCSPC) is used to determine time-domained fluorescence measurements, among these the fluorescence lifetime and a setup of the procedure is schematically presented in figure 3.3. The foundation of this technique is the time-to-amplitude converter (TAC) [25]. First an excitation pulse is sent out from the light source simultaneously starting the measurement clock and exciting the sample. This pulse starts a ramp voltage, for example by charging a ca-

pacitor, in the TAC which stops when fluorescence from the sample is detected. The TAC's output pulse has voltage which is proportional to time between start and stop.

The sample is repetitively hit with excitation pulses, and for each hit a multichannel analyzer (MCA) converts the voltage into a time channel. This is done with use of analog-to-digital converter. The MCA, summing over all the pulses, makes a histogram of counts versus time channels. It is common to let the measurement end when the peak channel hits 10000 counts to obtain enough signal to noise ratio. The fluorescence lifetime measurements were obtained using the Jobin Yvon IBH FluoroCube photon-counting spectrometer with a TBX-04 picosecond photon detection module. Horiba NanoLEDs were used as excitation sources. The data were analyzed using the IBH data analysis software.

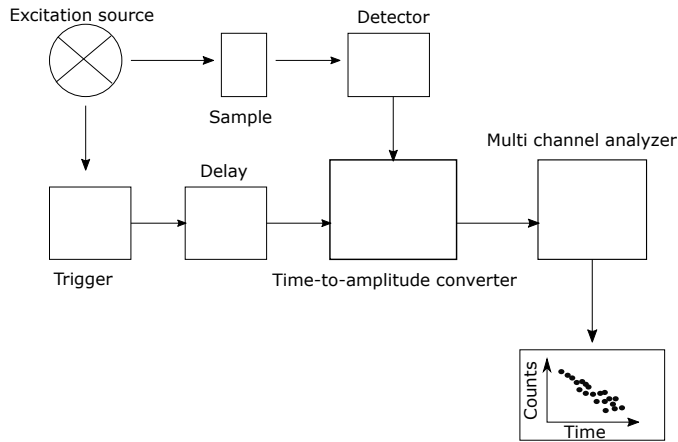


Figure 3.3: A schematic of the setup for time-correlated single-photon counting. The delay corrects for different path lengths of start and stop signal. A filter or monochromator may be placed in front of the sample.

The response functions of the excitation pulse and the system should ideally be  $\delta$ -functions, but these do not exist and are in fact comparable to the fluorescence lifetime [31]. The measured fluorescence decay curve  $F(t)$  is therefore a convolution of the theoretical impulse response function  $I(t)$  and the instrument response function  $L(t)$  yielding the convolution integral

$$F(t) = \int_0^t L(t') I(t - t') dt' \quad (3.2)$$

The software IHB data-analysis was used to calculate this convolution automatically and also provided the standard deviation of the measured lifetimes.

### 3.5 Excited state absorption spectroscopy

Excited state absorption is an extension of absorption spectroscopy in the sense that it measures the absorbance from the excited states  $S_1$  and  $T_1$ . It is an important technique to quantify triplet states when there is no or only weak phosphorescence emission. The way to achieve this is by using a technique known as flash photolysis. The principle is that the sample is first excited into the singlet manifold and synchronously a second flash is imposed, from which the spectral transition is measured [32]. If there is inter-system crossing (ISC) the excitation will end up in a triplet state with relative long life-time. By measuring the triplet absorption decay and assuming no triplet-triplet quenching processes the differential equation for the triplet concentration is as follows [20]:

$$\frac{dC_T}{dt} = -k_1 C_T \quad (3.3)$$

and solving the differential equation yields a single exponential decay solution

$$C_T = C_T(0) \exp^{-k_1 t}. \quad (3.4)$$

$C_T(0)$  the integration constant which is equal to the concentration triplets at zero time. or in terms of life time  $\tau_1 = \frac{1}{k_1}$ ,

$$C_T = C_T(0) \exp^{\frac{-t}{\tau_1}}. \quad (3.5)$$

The experimental setup is composed of both commercial products

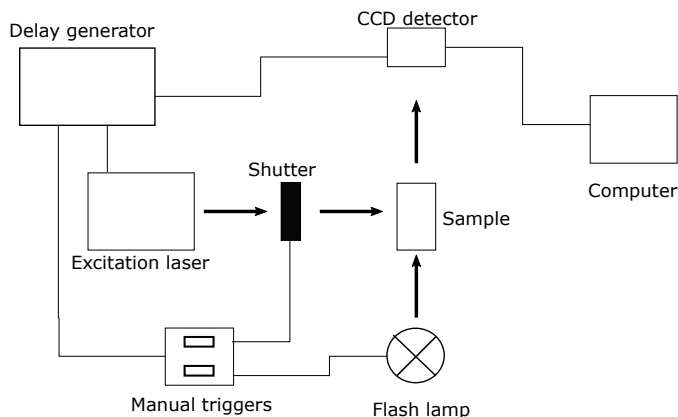


Figure 3.4: A schematic of the setup for excitation state absorption spectroscopy

and locally built units and the schematic is shown in figure 3.4. The excitation source was a NT 342B-SH-10-WW laser (Ekspla, Lithuania), array detector (Applied Photophysics, United Kingdom) and a xenon flash lamp module (Model L9456-01,5W, Hamamatsu, Japan) with BWSpec software (B&W Tek, USA). The samples were purged of oxygen by with the use argon gas, for minimum 8 minutes beforehand. The samples were measured to have an absorbance of 0.15 O.D. at 355 nm which is the excitation wavelength of the laser.

### 3.6 Singlet oxygen luminescence

Singlet oxygen have a distinct phosphorescence centered around 1270 nm [11, 13, 33]. This can be used to detect the presence of singlet oxygen as well as determining the singlet oxygen lifetime. The lifetime depends on the concentrations of molecules that are in the triplet excited state, the concentration of oxygen in the triplet ground state, the rate constant that forms the singlet oxygen and then finally rate constant that removes singlet oxygen. The concentration of singlet oxygen can be described by the equation

$$S(t) = S_0 \left( -\exp^{-k_r t} + \exp^{-k_\Delta t} \right). \quad (3.6)$$

$S_0$  contains the concentration of triplet ground state oxygen. The  $\tau_r = \frac{1}{k_r}$  and  $\tau_\Delta = \frac{1}{k_\Delta}$  are the rise time and the decay time, respectively. The former one describes how fast the oxygen reacts with the triplet excited state which creates singlet oxygen. The latter tells how fast the reactions which removes singlet oxygen works; in other words the singlet oxygen lifetime.

Singlet oxygen luminescence was detected by exciting the sample using a NT 342B-SH-10-WW laser (Ekspla, Lithuania) and an Infiniium 54830BDSU oscilloscope (Keysight, U.S.). A filter with transmittance centered around 1270 nm was placed in front of a photomultiplier tube (PMT) detector to only detect singlet oxygen phosphorescence, as shown in figure 3.5. In order to get a reference signal from the sample the solution was deoxygenated by purging the oxygen from the solution with argon gas for minimum 8 minutes. The samples were measured to have an absorbance of 0.15 O.D. at 355 nm which is the excitation wavelength of the laser.

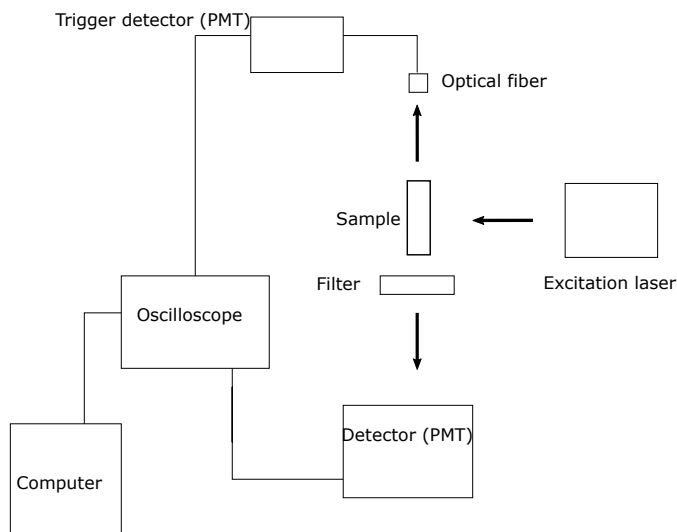


Figure 3.5: A schematic of the setup for detecting singlet oxygen.

### 3.7 Cultivation of cancer cells

In this thesis two cell lines were used, from rat (AY27) and human (WiDr). The AY27 cells are from rat bladder and originally provided by Professor Steven H. Selman (University of Toledo, Ohio, USA) [11]. The WiDr cells are derived from a human primary adenomacarcinoma from the colon, provided by Qian Peng (Oslo University Hospital, Oslo, Norway) [34]. The cells were grown in sterile cell culture flasks (75 cm<sup>2</sup>, Corning) and the cultivation medium used for the AY27 cells was Roswell Park Memorial Institute (RPMI) 1640 Medium. The 500 ml medium was supplemented with 50 ml fetal bovine serum (FBS), 1.7 ml L-glutamine and 5.0 ml penicilin/streptomycin.

The WiDr cultivation medium was Roswell Park Memorial Institute 1640 Medium with additional glutamine. The 500 ml medium was supplemented with 50 ml fetal bovine serum (FBS), 1.7 ml L-glutamine and 5.0 ml penicilin/streptomycin. A solution of phosphate-buffered saline (PBS) was used for washing the cells before detachment. The culture medim, FBS, glutamin and trypsin were all aquired from Gibco BRL, Life Technologies, (Inchinnan, Scotland).

The cells were incubated in an environment of 95% humidified air and 5% CO<sub>2</sub> in 37 °C When not used for experiments the cells were regularly checked upon (for infections etc.) by using a microscope for evaluation of the cell conditions. These conditions are important to know before changing medium or splitting cells. The medium change was done when the medium had changed color from bright red to yellow as it was an indication that the cells had consumed the nutrients in the medium.

Cell splitting was performed when the culture flasks were 80-100% confluent. This was done by removing old medium, washing with (PBS, 5 ml) and adding trypsin (3 ml). The culture flask (75 cm<sup>2</sup>) with trypsin was placed in the incubator for 2-3 minutes and then checked in the microscope to see if all cells were detached. To ensure that all the cells were detached, the flask was tapped against a hard surface until all cells were detached. Growth medium (7ml) was then added to the flask before

transferring (9 ml) of the solution to a centrifugal tube (Corning). The remaining volume of the solution was used to determine the concentration of cells by counting the number of cells in a Bürker chamber. Then the solution in the centrifugal tube was centrifuged at 1500 rpm for 5 minutes. The supernatant was removed and new medium was added to the precipitate until a solution with a desired concentration was achieved. This concentration depends on the cell type and if the cells have to be used for an experiment or just for subculturing.

### **3.8 Cell survival assay (MTT)**

After the cells were treated with PS they were incubated for 24 hours when checking the viability of the cells for different concentration of PS. The cells which were going to be treated with light were incubated for 48 hours.

The 3-(4,5-dimethylthiazol-2-yl)-2,5-diphenyltetrazolium bromide (MTT) working solution with concentration 0.5 mg/ml was prepared by adding MTT stock solution (5 mg/ml) and growth medium in a 50 ml Corning centrifugal tube. The tube was covered with aluminum foil and heated to 37 °C in a water bath. The old medium in the cell dishes was removed before washing (PBS, 3 ml, 37 °C). After that MTT working solution (2 ml) was added. After one hour incubation at 37 °C the working solutions were removed and isopropanol was added carefully. The cell dishes with isopropanol were placed on a shaker at approximately 300 rpm for 30 minutes. Afterwards the solutions were transferred to centrifugation tubes and centrifuged at 1500 rpm for 5 minutes. The supernatant was transferred to cuvettes and the absorption was measured at 595 nm by using a single beam spectrophotometer (UV-1201 Shimadzu, Kyoto, Japan). The cell viability was determined using the untreated cells as a positive control.

### 3.9 Photobleaching experiment

All the living WiDr cell-samples were provided by the co-supervisor Odrun A. Gederaas (Department of Chemistry, NTNU, Trondheim, Norway) as follows: First, a culture of WiDr cells were seeded to the concentration of 2.0 million cells per 6 cm-dish in regular cultivation medium. Thereafter the dishes were washed with PBS, before treated with a medium containing 2.5  $\mu\text{M}$  PS in the dark. The PS The cells were then left in an incubator (37 °C) for 24 hours. The cells were retrieved and exposed to blue light ( $\lambda = 435 \text{ nm}$ , LumiSource see appendix B) for different time intervals (0 s, 30 s, 60 s, 120 s and 600 s). There were also control samples without PS or light (dark toxicity). The fluorescence intensity for each time interval was plotted and compared to each other.

### 3.10 Photodynamic treatment of erythrosin B and gold nanoparticles

The AY27 cells were seeded out to the concentration of 0.5 million cells per 6 cm-dish in regular medium and were incubated (37 °C) for 24 hours before adding the different concentrations of erythrosin B and gold nanoparticles (see appendix C for technical details). The cells were incubated for another 24 hours, washed with PBS multiple times and exposed to green light in PBS (3 ml) ( $\lambda = 532 \text{ nm}$ ). The setup is shown in figure 3.6). It consists of an laser (Suwtech LDC 1500, China) a lens focusing the beam from the laser into a fiber which illuminates an area which is approximately homogeneous. The intensity of the laser was determined by measuring the effect using a Fieldmaster GS (Coherent, USA). The area which the dish is placed is marked with a white card taped to remain stationary. The cells were exposed to the following time intervals: 12 min, 24 min and 36 min corresponding to 4 J/cm<sup>2</sup>, 8 J/cm<sup>2</sup> and 12 J/cm<sup>2</sup>, respectively.

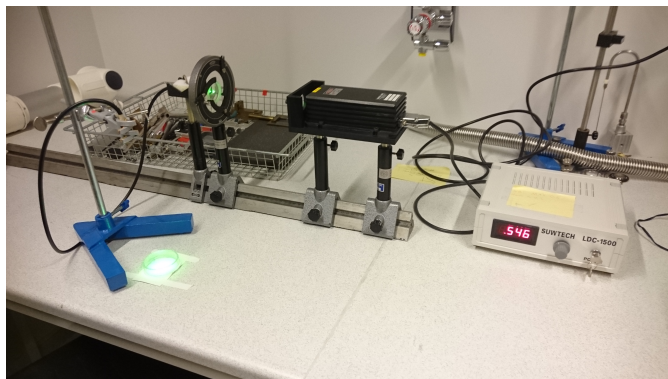


Figure 3.6: A picture of the setup used to expose the cells treated with erythrosin B and gold nanoparticle to green light ( $\lambda = 532$  nm).

### 3.11 Preparation of samples

The gold nanoparticles, and gold-loaded lipid nanoparticles were provided by PhD student Andreia Granja from the University of Porto, Portugal. Structural information is given in appendix C.

All stock solutions of samples and reference molecules were made by dissolving powders in the appropriate solvent. These powders were obtained from two companies, Fluka and Sigma Aldrich. The samples that were from Sigma Aldrich are eosin B, erythrosin B, perinaphthenone and tetraphenylporphyrin. The ones from Fluka were quinine sulfate and fluorescein. The powder was weighed on a microbalance MT5 (Mettler Toledo, Ohio, U.S) and the amount of solvent was added by using a pipette, yielding the desired concentration<sup>1</sup>. The structural of eosin B, erythrosin B and perinaphthenone are all given in appendix C.

The photosensitizers used in this thesis are intellectual property and have been given uncompromising names along with no structural details<sup>2</sup>.

---

<sup>1</sup> The stock solutions of perinaphthenone and eosin B were provided by supervisor Mikael Lindgren

<sup>2</sup> All the photosensitizers were provided by Christine Contino-Pépin, Université d'Avignon et des pays de Vaucluse. The stock solutions were provided by co-supervisor Odrun A. Gederaas

The structural information of the gold nanoparticles and gold-loaded lipid nanoparticles is given in appendix C.

In all the absorption and fluorescence experiments 3 ml quartz cuvettes were used as sample cells with a path length of 1 cm.

## 3.12 Estimation of errors

A part of doing experimental work is to take into account errors and uncertainties. Errors can be calculated manually, using a specific software, or using a combination of the two. In this thesis both are done with some simplifications for a selection of the photophysical properties determined. The uncertainty of the values for the absorption coefficient and the quantum yield are calculated using the methods explained later in this chapter. The values of fluorescence are not of any importance except for the integrated value for the quantum yield, the error associated with these measurements will be included, when calculating the error of the quantum yield value. The fluorescence lifetime analysis software provided the standard deviation. For the triplet state decay measurements and singlet oxygen luminescence no uncertainty are calculated but a plot of residuals in both measurements are used to say something about the reliability of resulting values.

### 3.12.1 General error calculation

All measurements have a uncertainty associated with them, for instance when measuring the values  $q$ ,  $r$  and  $s$  they will have uncertainties denoted by  $\delta q$ ,  $\delta r$  and  $\delta s$ . A quantity  $T$  calculated depending on those measurements will have a uncertainty will "propagate" to the quantity  $T$  [35]. Under the assumption that the quantities  $\delta q$ ,  $\delta r$  and  $\delta s$  have random and uncorrelated errors. If the relation between  $T$  and the measurements are

$$T = \frac{qrs}{tuv}, \quad (3.7)$$

or

$$T = q + r + s + \dots - (t + u + v) \quad (3.8)$$

the uncertainty of  $T$  can be expressed as

$$\frac{\delta T}{|T|} = \sqrt{\left(\frac{\delta q}{q}\right)^2 + \left(\frac{\delta r}{r}\right)^2 + \left(\frac{\delta s}{s}\right)^2 + \left(\frac{\delta t}{t}\right)^2 + \left(\frac{\delta u}{u}\right)^2 + \left(\frac{\delta v}{v}\right)^2}. \quad (3.9)$$

Which is the formula If  $T = q^n$  then the equation for the uncertainty is

$$\frac{\delta T}{|T|} = |n| \frac{\delta q}{|q|}. \quad (3.10)$$

### 3.12.2 Error in calculation of gradient in quantum yield

The gradient is a straight line described by the general equation  $y = mx + b$ , and the fit is the best line going through the experimentally measured points. The standard statistical method to get this fit is to use the method of least squares. The best values for  $m$  and  $b$  are the ones when the function

$$S = \sum (y_i - mx_i - c)^2 \quad (3.11)$$

is a minimum and which why it is called method of least squares [36]. The values of  $m$  and  $c$  can then be found by solving the equations

$$\frac{\partial S}{\partial m} = 0 \quad (3.12)$$

$$\frac{\partial S}{\partial c} = 0 \quad (3.13)$$

which after several steps yields the best values for  $m$  and  $c$  given by

$$m = \frac{\sum (x_i - \bar{x}) y_i}{\sum (x_i - \bar{x})^2} \quad (3.14)$$

and

$$c = \bar{y} - m\bar{x}. \quad (3.15)$$

$\bar{x} = \frac{1}{n} \sum x_i$  and  $\bar{y} = \frac{1}{n} \sum y_i$  which tells us that the best fit has a line going through the center of gravity of the points.

All the fitted lines are retrieved from the "fit" function in gnuplot.

### 3.12.3 Uncertainty of the quantum yield

The error propagation of equation 3.1 with the use equations 3.9 and 3.10 yields the equation of uncertainty for the quantum yield

$$\frac{\delta \Phi_S}{|\Phi_S|} = \sqrt{\left(\frac{\delta \Phi_{Ref}}{\Phi_{Ref}}\right)^2 + \left(\frac{\delta m_S}{m_S}\right)^2 + \left(\frac{\delta m_{ref}}{m_{Ref}}\right)^2 + 4\left(\frac{\delta n_s}{n_s}\right)^2 + 4\left(\frac{\delta n_{Ref}}{n_{Ref}}\right)^2} \quad (3.16)$$

where  $m_S$  and  $m_{Ref}$  are the gradients for the sample and reference, respectively. The constant term  $c$  have here been disregarded as it is far too complicated to calculate and an estimation of it would serve the same purpose.

### 3.12.4 Instrumental errors

According to the manufacturer of the spectrophotometer used for absorption spectroscopy the accuracy of the absorption measurements are  $\pm 0.004 \text{ abs}$  [37]. The accuracy of the scale, MT5 (Mettler Toledo, U.S.) is dependent on the geographical location and height over sea level [38]. For simplicity the accuracy is set to the same as the linearity of  $\pm 4 \mu\text{g} = \pm 0.004 \text{ mg}$ . The pipettes used to make the compound solutions were one Finnpiptette 5-40  $\mu\text{L}$  (Thermo Scientific, U.S.) and four Transferpettes with the volumes 20  $\mu\text{L}$ , 200  $\mu\text{L}$ , 1000  $\mu\text{L}$  and 5 ml (Brand, Germany). According to the web pages for these two pipette brands the typical error is 1% [39, 40]. Due to the condition of the pipettes this error is estimated to be twice that of the manufacturers.

### 3.12.5 Uncertainty of the cell viability

The cell viability measurements are all done multiple times and for each distinct measurement, either light dose or concentration. The points plotted are the mean value of those experiments and the errorbars are the standard deviation. These values are achieved using the "stats"-function in gnuplot. The mathematical equation for the standard deviation, is

$$STD = \sqrt{\frac{1}{N} \sum (y_i - \bar{y})^2}, \quad (3.17)$$

Where N is the number of measurements,  $y_i$  is the value i-th measurement and  $\bar{y}$  is the mean of the measured values [41].

# Chapter 4

## Results

### 4.1 Photophysical properties of tested PS

Several compounds were tested as potential photosensitizers in this master's thesis. The basic photophysical properties were characterized. In addition the existence of excited state absorption was verified for several of the compounds. The compounds that exhibited triplet excited state absorption were investigated further in terms of triplet state decay time. Finally, the ability to produce singlet oxygen was also investigated. The most important basic photophysical properties of the reference compounds and samples are summarized in tables 4.1, and 4.3, respectively.

#### 4.1.1 Absorption spectra

As the main objective of PDT is to destroy cancerous cells by creating singlet oxygen and ROS. The PS must absorb in the ultraviolet and or visible light and transfer energy efficiently to the triplet states. Shown in figure 4.1 are the absorption spectra of the three compounds erythrosin B, eosin B and perinaphtenone. Erythrosin B has a band in which it absorbs from around 450 nm to 560 nm with a peak at 533 nm. Eosin B has two absorption bands, a small one from around 360 nm to 440 nm and a

larger from 450 nm to 560 nm with a peak around 522 nm, which is in the same range as erythrosin B. Perinaphtenone on the other hand showed a band from 300 nm to around 445 nm, with a peak at 360 nm.

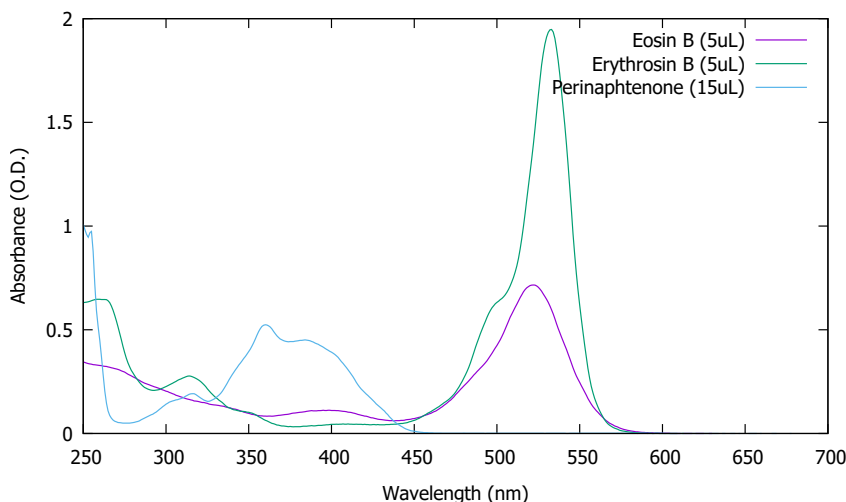


Figure 4.1: Absorption spectra of perinaphtenone, eosin B and erythrosin B. The two 5  $\mu\text{L}$  and the one 15  $\mu\text{L}$  is how much stock solution of the compound were added to 3 ml of tetrahydrofuran (THF) dilute. This is to visualize the relationship between absorption and amount of stock solution for the three samples. 15  $\mu\text{L}$  was used due to poor signal for lower concentrations

Three protoporphyrins compounds were also characterized: PpIX, Protoporphyrin A (PpA) and Protoporphyrin B (PpB), for which the absorption spectra are shown in figure 4.2. Both PpA and PpB have the same absorption bands and peaks, with a large Soret peak at 400 nm and smaller Q-bands with peaks around 498 nm, 531 nm, 569 nm and 624 nm. PpIX have a small redshift of its spectrum compared to PpA and PpB with the Soret peak at 405 nm and the Q-bands with their peaks at 505 nm, 538 nm, 577 nm and 633 nm. These spectra are typical for porphyrins [42, 43]

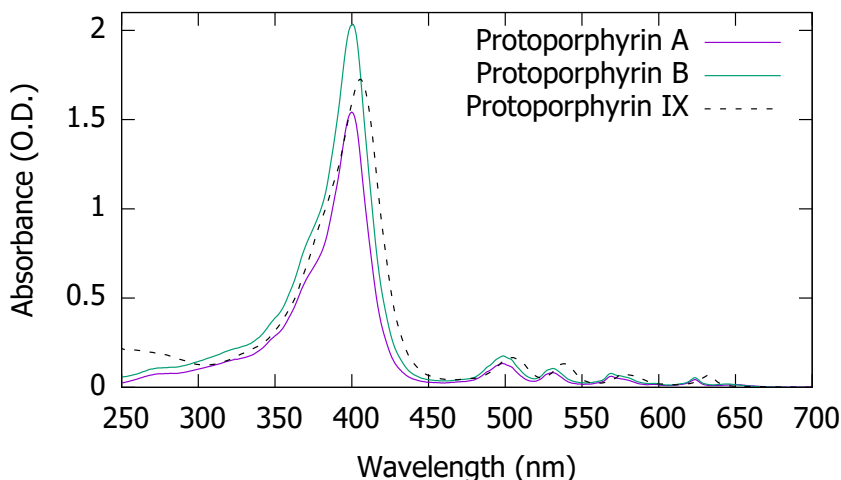


Figure 4.2: Absorption spectra of PpA, PpB and PpIX. The concentration is equal for the three samples.

#### 4.1.2 Fluorescence spectra

The fluorescence spectra were used to determine the quantum yield and lifetime of the respective compounds. The fluorescence spectra of erythrosin B, eosin B and perinaphtenone were also measured with and without the purging of oxygen from the sample. The fluorescence spectra of perinaphtenone in figure 4.3a, shows that for  $\lambda_{Ex} = 360$  nm the peak was slightly shifted compared to the peak of the deoxygenated sample. There is also a shift in the peak if the excitation wavelength is changed from 360 nm to 420 nm, being located at around 425 nm and 500 nm, respectively. The absorption peak is not shifted for the deoxygenated sample when exciting at 420 nm, located around 500 nm.

The fluorescence spectra for eosin B and erythrosin B, did not show any differences in fluorescence after deoxygenating. Neither of the protoporphyrins were deoxygenated, and all spectra are shown in figure 4.4. The fluorescence peaks of PpA and PpB are located at the same wavelengths with the peaks of PpIX being slightly red shifted in comparison. The fluorescence of PpB is stronger when compared to PpIX and PpA in the 610-725 nm region. When comparing PpIX and PpA, PpIX shows

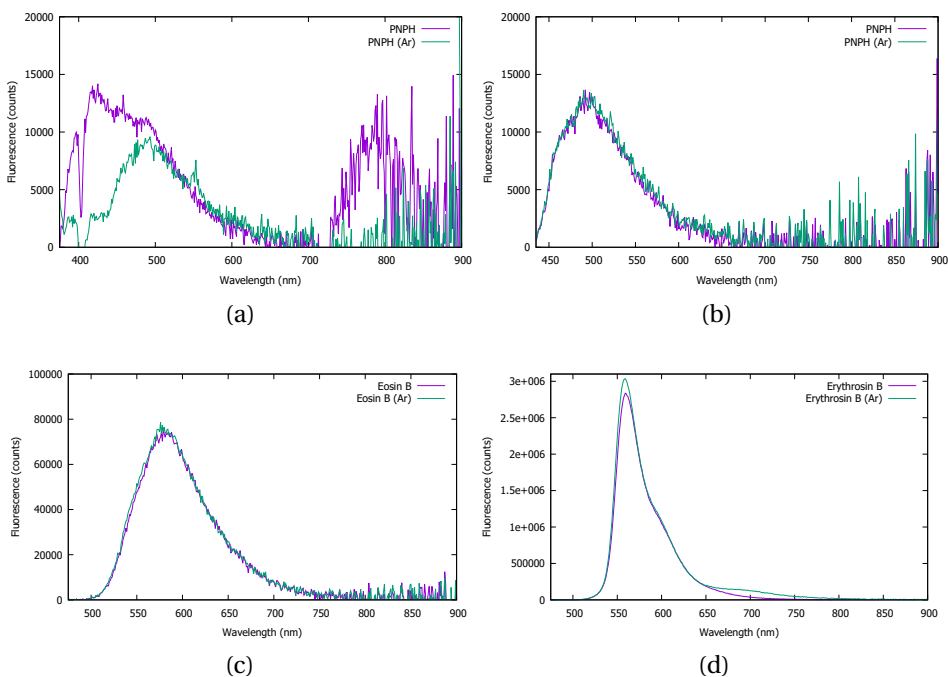


Figure 4.3: Fluorescence spectra of:(a) Perinaphtenone excited at 360 nm, (b) perinaphtenone excited at 420 nm, (c) eosin B and (d) erythrosin B. The deoxygenated solutions are plotted in green and the solutions with oxygen are plotted in purple.

Table 4.1: Absorption characteristics of the sample compounds investigated.  $\lambda_{Abs}$  is the wavelength which yielded maximum absorption,  $\epsilon$  the molar extinction coefficient and lastly which solvent was used to make the sample solution.

Sample	$\lambda_{Abs}$ (nm)	$\epsilon$ ( $10^5 \text{M}^{-1} \text{cm}^{-1}$ )	Solvent
Erythrosin B	533	1.17	THF
Perinaphtenone	360	1.05	THF
Eosin B	522	4.30	THF
Protoporphyrin IX	405/406	1.71	THF
Protoporphyrin A	400	15.6	THF
Protoporphyrin B	400	20.6	THF

a stronger fluorescence in blue end of the spectrum, while PpA is has stronger fluorescence in the red end of the spectrum.

The spectra shown in figures 4.3-4.4 were used to determine the wavelengths used to obtain the fluorescence lifetime and quantum yield values summarized in table 4.3.

Table 4.2: Photophysical characteristics of the reference compounds used to investigate the samples.  $\lambda_{Abs}$  is the wavelength of maximum absorption,  $\lambda_{Fl}$  is the wavelength of maximum fluorescence,  $\Phi_{Fl}$  is the fluorescence quantum yield and  $\tau_{FL}$  is the fluorescence lifetime.

Reference sample	$\lambda_{Abs}$ (nm)	$\lambda_{Fl}$ (nm)	$\Phi_{Fl}$	$\tau_{FL}$ (ns)
Quinine Sulfate	316	454	$0.52 \pm 0.02$ <sup>1</sup>	$19.87 \pm 0.07$
Fluorescein	490	514	$0.91 \pm 0.05$ <sup>2</sup>	$4.12 \pm 0.09$ <sup>3</sup>
Tetraphenylporphyrin	419	652	$0.13 \pm 0.01$ <sup>4</sup>	$12.40 \pm 0.06$

<sup>1</sup> [44]<sup>2</sup> [45]<sup>3</sup> [46]<sup>4</sup> [47]

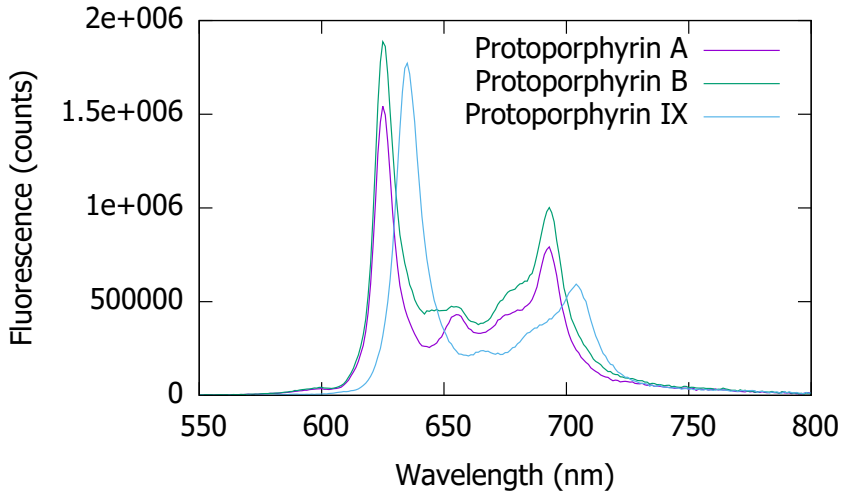


Figure 4.4: Fluorescence spectra of PpA, PpB and PpIX.

Table 4.3: Fluorescence characteristics of the sample compounds investigated.  $\lambda_{Fl}$  is the wavelength of maximum fluorescence,  $\Phi_{Fl}$  is the fluorescence quantum yield and  $\tau_{FL}$  is the fluorescence lifetime.

Sample	$\lambda_{Fl}$ (nm)	$\Phi_{Fl}$	$\tau_{FL}$ (ns)
Erythrosin B	559	0.70( $\pm$ 0.06)	n.d.
Perinaphtenone	500(425)	n.d.	36.52 $\pm$ 0.04*
Eosin B	588	0.02 $\pm$ 1.34	n.d.
Protoporphyrin IX	635	0.09 $\pm$ 0.39	10.13 $\pm$ 0.09
Protoporphyrin A	625	0.09 $\pm$ 0.39	13.46 $\pm$ 0.05
Protoporphyrin B	625	0.07 $\pm$ 0.40	13.57 $\pm$ 0.05

<sup>6</sup> [48]   <sup>7</sup> [48]   <sup>8</sup> [48]   <sup>9</sup> [48]   <sup>10</sup> [48]   <sup>11</sup> [49]   <sup>12</sup> [50]   <sup>13</sup> [51]

Table 4.4: Summary of the values used when determining the quantum yield.  $\lambda_{Ex}$  is the excitation wavelength and  $n_D$  is the refractive index of solvent used for to make the sample/reference.

Sample/reference	$\lambda_{Ex}$ (nm)	solvent	$n_D$
Erythrosin B	470	THF	$1.40468 \pm 0.00002$ <sup>5</sup>
Perinaphthenone	350	THF	$1.40468 \pm 0.00002$ <sup>6</sup>
Eosin B	350	THF	$1.40468 \pm 0.00002$ <sup>7</sup>
Protoporphyrin IX	514	THF	$1.40468 \pm 0.00002$ <sup>8</sup>
Protoporphyrin A	514	THF	$1.40468 \pm 0.00002$ <sup>9</sup>
Protoporphyrin B	514	THF	$1.40468 \pm 0.00002$ <sup>10</sup>
Quinine Sulfate	350	H <sub>2</sub> SO <sub>4</sub>	$1.41827 \pm 0.01$ <sup>11</sup>
Tetraphenylporphyrin	514	TOL	$1.5059 \pm 0.0002$ <sup>12</sup>
Fluorescein	470	NaOH	$1.474 \pm 0.001$ <sup>13</sup>

### 4.1.3 Fluorescence lifetime

The fluorescence decay, measured as a function of time, is given in figure 4.5. The excitation wavelength for PpA, PpB and PpIX is 403 nm and 337 nm for perinaphthenone. The emission wavelengths used are 625 nm for PpA and PpB, 635 nm for PpIX and 555 nm for perinaphthenone. The calculated values for the fluorescence lifetime,  $\tau_{Fl}$ , are all given in table 4.3.

### 4.1.4 Quantum yield

All the values found for the quantum yield are given in figure 4.3. The measurements have been done once for all the samples during this thesis. The plot of the gradients found are given in figures 4.6 and 4.7. The protoporphyrins all have a quantum yield 0.09 and erythrosin B was around 0.70. The luminescence of eosin B and perinaphthenone was very weak and it was not possible to determine a quantum yield.

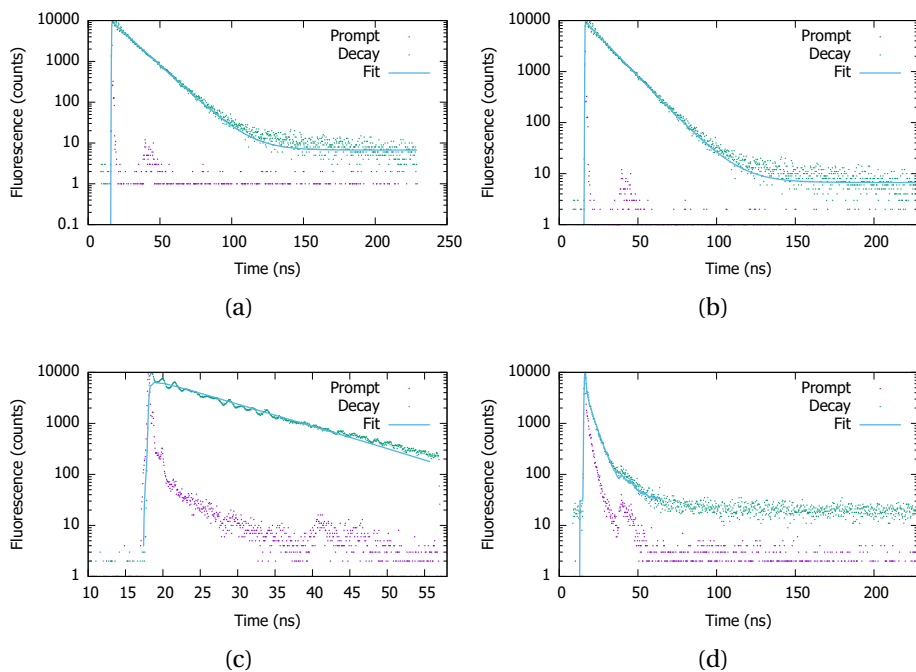


Figure 4.5: Fluorescence decay of:(a) PpA in THF,  $\lambda_{Ex} = 403$  nm  $\lambda_{Em} = 625$  nm, (b) PpB in THF,  $\lambda_{Ex} = 403$  nm  $\lambda_{Em} = 625$  nm, (c) PpIX in THF  $\lambda_{Ex} = 403$  nm  $\lambda_{Em} = 635$  nm and (d) Perinaphthenone in THF  $\lambda_{Ex} = 337$  nm  $\lambda_{Em} = 555$  nm.

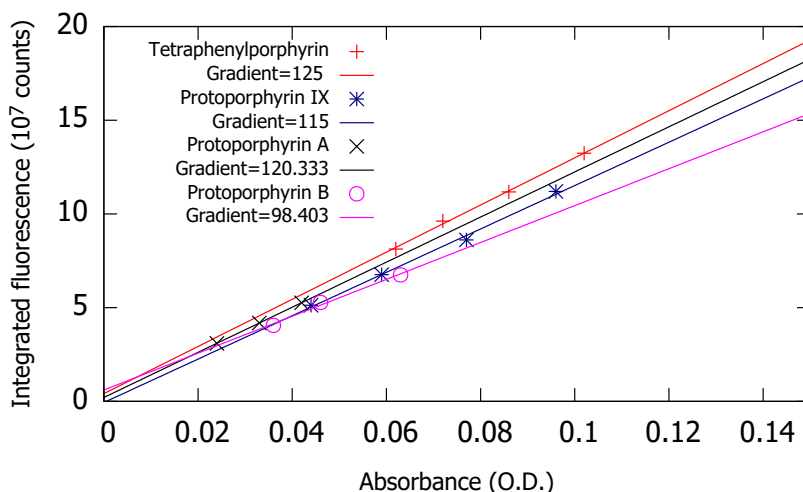


Figure 4.6: Relative quantum efficiency gradient plots for tetraphenylporphyrin, PpA, PpB and PpIX.

#### 4.1.5 Excited state absorption

The pump and probe measurements of all the samples was used to confirm triplet excited state absorption. (For more details see section 5.3.1). All those which were measured (except eosin B) showed absorption to the triplet states as shown in figures 4.8 and 4.9. The signal from the protoporphyrins shows a strong absorption from 420 nm to 500 nm and then weaker absorption bands between 500 nm and 800 nm. The signal gets weaker as the delay between excitation and detection is increased.

Erothrysin B showed a small triplet absorption band around 340 nm and a large band from 550 nm to 900 nm. The signal from perinaphthenone showed triplet absorption bands in the regions of 320-350 nm and 420-520 nm.

In addition, the triplet state decay was measured and analyzed by a Matlab script and the triplet lifetime was determined from the decay of the absorption by varying the time of the gated detection. The value of the lifetimes are shown in 4.5. The samples were excited at various wavelengths, averaged for different number of flashes and a were exposed to air. Representative plots of triplet state decay are given in figures 4.10-

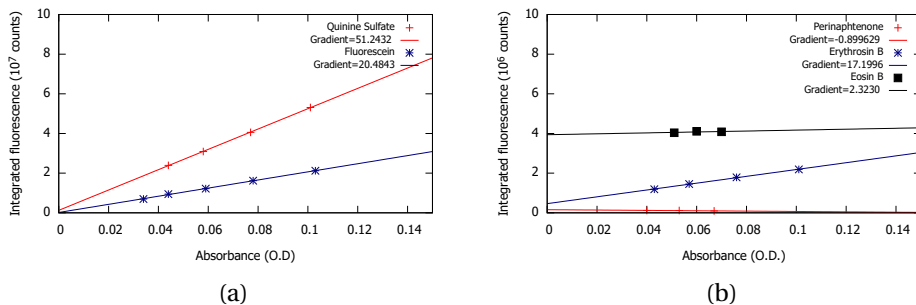


Figure 4.7: Relative quantum efficiency gradient plots of the: (a) Reference compounds quinine sulfate and fluorescein, (b) sample compounds eosin B, perinaphthenone and erythrosin B.

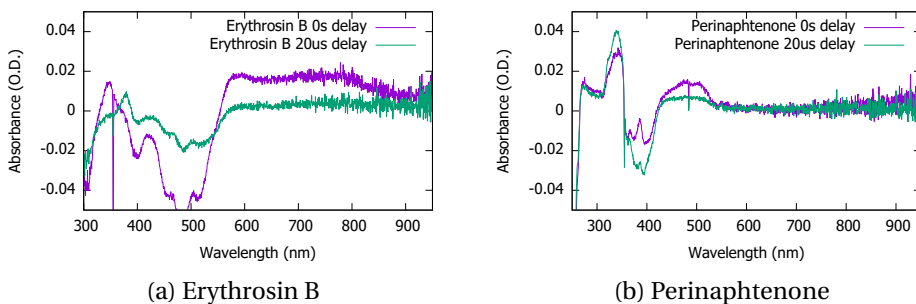


Figure 4.8: Plot of the excited state absorption spectra of erythrosin B and perinaphthenone with and without delay of flashlamp with respect to laser.

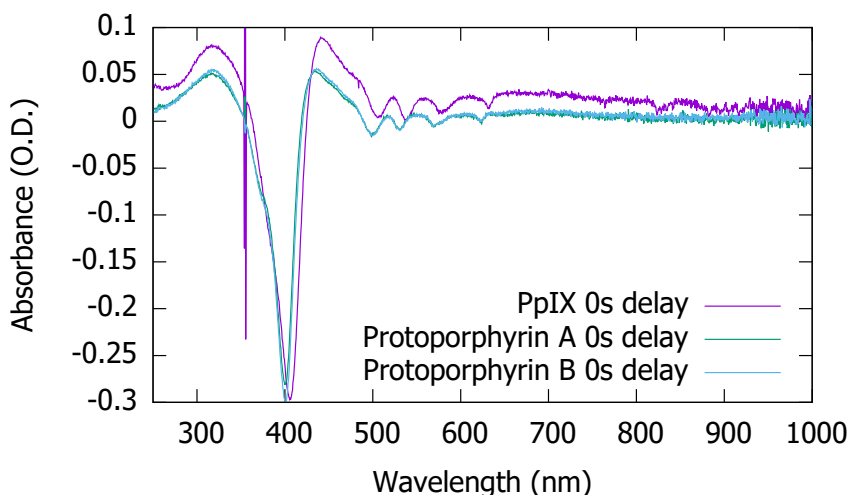


Figure 4.9: Plot of excited state absorption spectra of PpA, PpB and PpIX.

4.12 and fitted data are given in table 4.5. (Remaining plots are shown in appendix A).

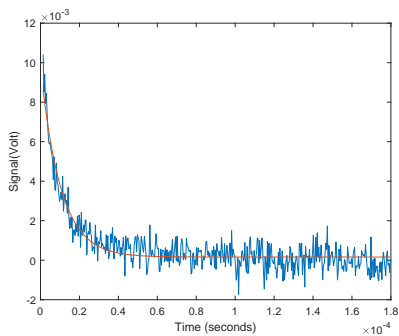
#### 4.1.6 Singlet oxygen measurements

Representative plots of time-resolved singlet oxygen luminescence are shown in figure 4.13-4.15 and all fitted data are shown in table 4.6 (remaining plots are shown in appendix A).

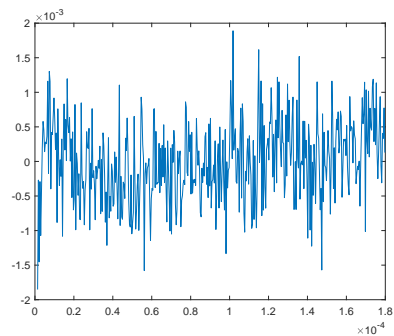
## 4.2 Viability & PDT results

### 4.2.1 Photobleaching measurements to assess PDT of protoporphyrins

The fluorescence measurements of the protoporphyrins were done in a dark environment and the treated cells were covered with aluminum in order to not expose them to uncontrolled light. When measuring the excitation wavelength was set to  $\lambda_{Ex} = 410$  nm. The results shown in figures 4.16 and 4.17, are the fluorescence measurements from the cells

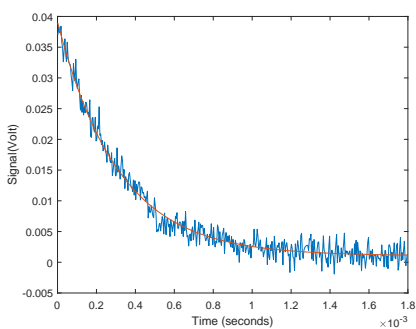


(a)

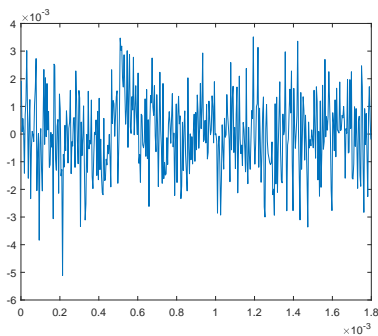


(b)

Figure 4.10: Plot of the: (a) Triplet state decay of erythrosin B measured at 600 nm. (b) Residual of the fit



(a)



(b)

Figure 4.11: Plot of the: (a) Triplet state decay of PpA measured at 435 nm. (b) Residual of the fit.

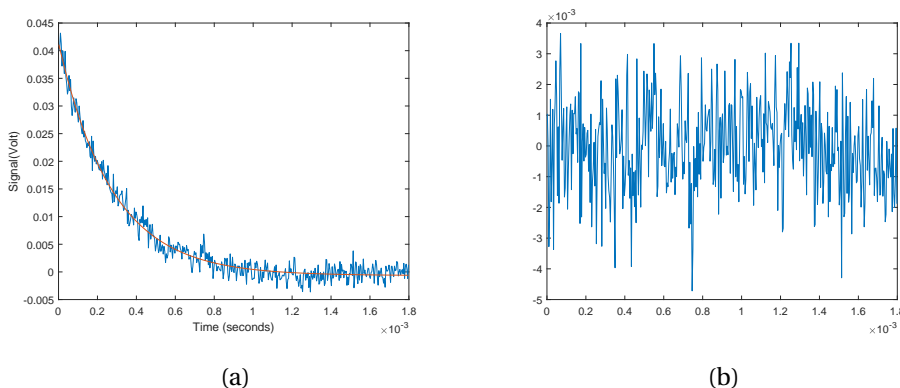


Figure 4.12: Plot of the: (a) Triplet state decay of PpB at 435 nm. (b) Residual of the fit.

Table 4.5: Excited state decay properties of the samples investigated.  $C_T(0)$  is the concentration of excited state molecules at time  $t = 0$  and  $\tau_T$  is the lifetime of the triplet excited state. The asterisk marks compounds which were oxygenated.

Sample	$C_T(0)$	$\tau_T$ $\mu s$
Erythrosin B*	0.02	0.71
Erythrosin B	0.01	10.36
Perinaphtenone*	0.01	0.72
Perinaphtenone	0.01	17.29
Protoporphyrin IX*	>0.01	1.28
Protoporphyrin IX	>0.01	18.58
Protoporphyrin A*	0.04	181.19
Protoporphyrin A	0.04	301.44
Protoporphyrin B*	0.37	10.92
Protoporphyrin B	0.42	274.86

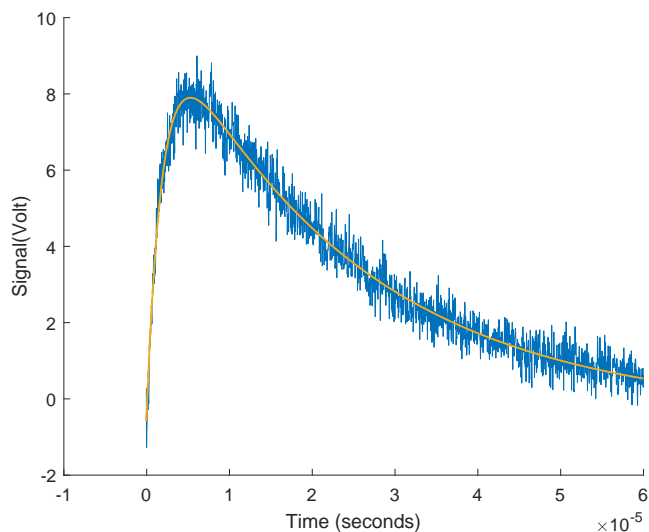


Figure 4.13: Plot of singlet oxygen luminescence from PpA analyzed by Matlab and fitted to determine the rise time and lifetime.

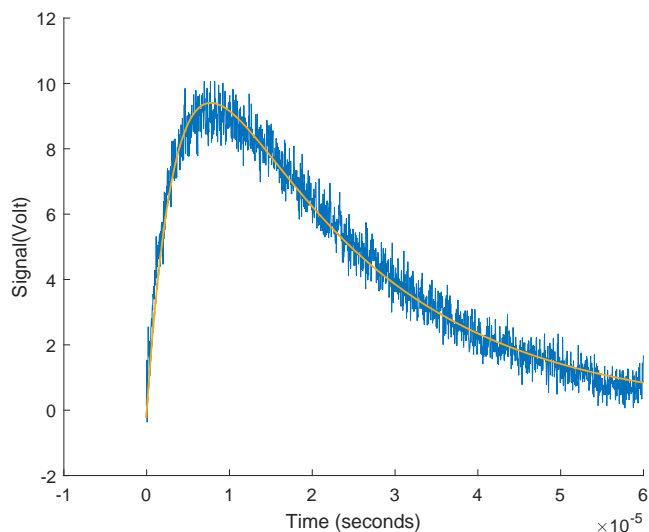


Figure 4.14: Plot of singlet oxygen luminescence from PpB analyzed by Matlab and fitted to determine the rise time and lifetime.

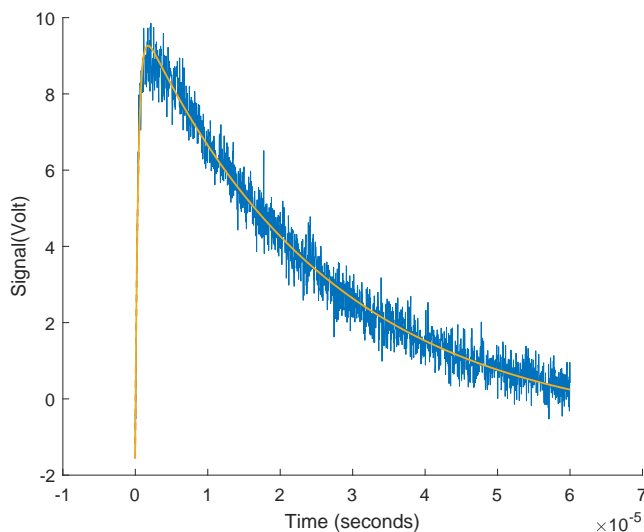


Figure 4.15: Plot of singlet oxygen luminescence from PpIX analyzed by Matlab and fitted to determine the rise time and lifetime.

treated with different light doses and indicates a trend, both PpA and PpB shows a decrease in fluorescence intensity at all the three peaks located at around 625 nm, 660 nm and 690 nm. When looking at the intensity of the fluorescence both the PS's they both start around 1.4 million in relative intensity for no light. Cells treated with PpA (2.5  $\mu\text{M}$ , 24 hours) appears to lose intensity faster than cells treated with PpB (2.5  $\mu\text{M}$ , 24 hours) for the the smaller doses. However at 1.55 J/cm<sup>2</sup>, there is a rather large drop of intensity for PpB, being close to half the intensity of PpA at the same light dose.

#### 4.2.2 The effect of gold nanoparticles

In order to see if the effect of PDT could be influenced by nanoparticles, the toxicity of the gold nanoparticles and the gold-loaded lipid nanoparticles were determined with MTT-assays. The results of three separate assays is shown in figure 4.20. The results show that the compounds have a high cell viability for low concentrations of the compounds, with a via-

Table 4.6: Singlet oxygen properties of the sample compounds investigated.

Sample	$S_0$	$\tau_r$ ( $\mu$ s)	$\tau_\Delta$ ( $\mu$ s)
Erythrosin B	5.34	0.47	11.17
Erythrosin B (with gold nanoparticles)	3.66	0.90	8.95
Perinaphtenone	18.95	1.05	13.97
Protoporphyrin IX	11.36	0.46	27.21
Protoporphyrin A	12.22	1.93	23.74
Protoporphyrin B	16.98	3.80	20.43

bility of 90% at 10  $\mu$ g/ml for the gold nanoparticle and 80% at 50  $\mu$ g/ml for the gold-loaded lipid nanoparticles.

When characterizing the photophysical properties of erythrosin B, a small amount (300  $\mu$ l) of gold nanoparticles were added to the stock solution to see if the nanoparticles had any influence on the phototherapeutic effect. The absorption spectrum of the gold nanoparticles showed no traditional absorption, but a phenomenon known as surface plasmon resonance [52]. This is shown in figure 4.21 along with the absorption spectra of erythrosin B with and without nanoparticles. A integrating sphere was used to collect the potential scattered light from the particles, but there was no significant difference between the two measurements.

### 4.2.3 PDT light treatment with gold nanoparticles

Erythrosin B was chosen to be used in a PDT light experiment to investigate its potential as a photosensitizer. The different parameters were three light doses, three different concentrations of erythrosin B and some cell dishes had gold nanoparticles added.

The concentration was 0.005  $\mu$ g/ml of gold nanoparticles, since that concentration yielded 100% cell viability according to figure 4.20. There are three variables, the light dose, the concentration of erythrosin B and

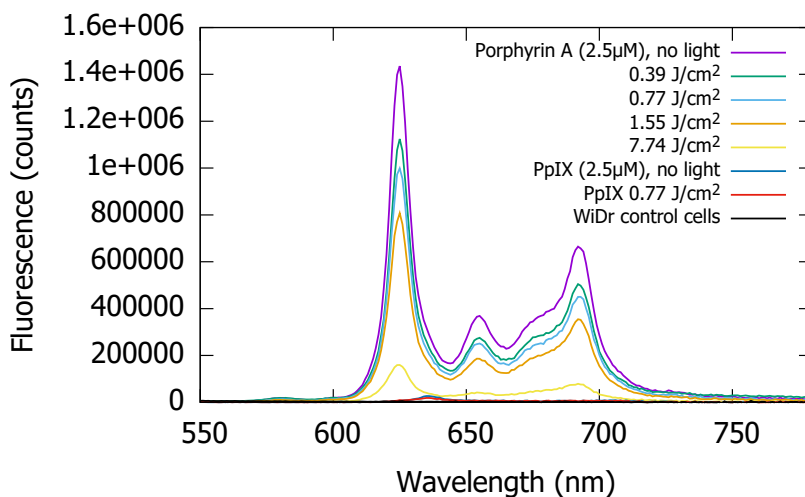


Figure 4.16: Plot of fluorescence spectrum for PpA, PpIX and control cells as a function of wavelength.

the presence or absence of gold nanoparticles. In figure 4.22 there are two sets of dishes with three concentrations of erythrosin B in each set, the difference is that one has gold nanoparticles added while the other has not.

The effect of gold nanoparticles is shown in 4.23 checked for three different light doses  $4 \text{ J/cm}^2$ ,  $8 \text{ J/cm}^2$  and  $12 \text{ J/cm}^2$ .

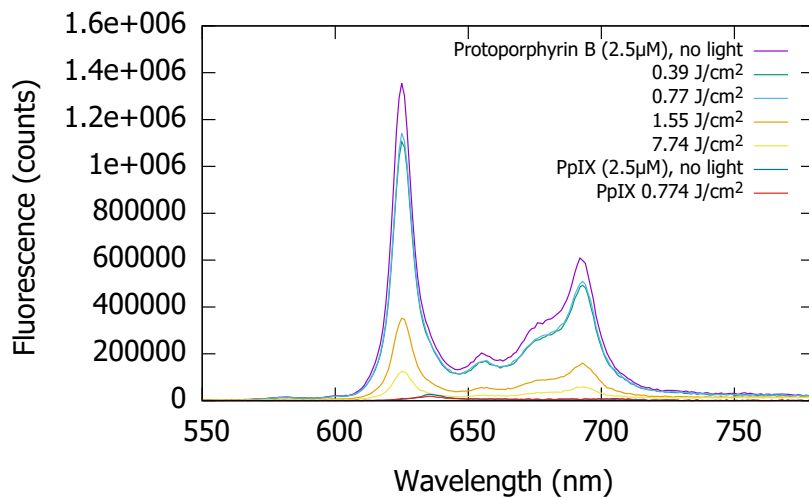


Figure 4.17: Plot of fluorescence spectrum for PpB and PpIX as a function of wavelength.

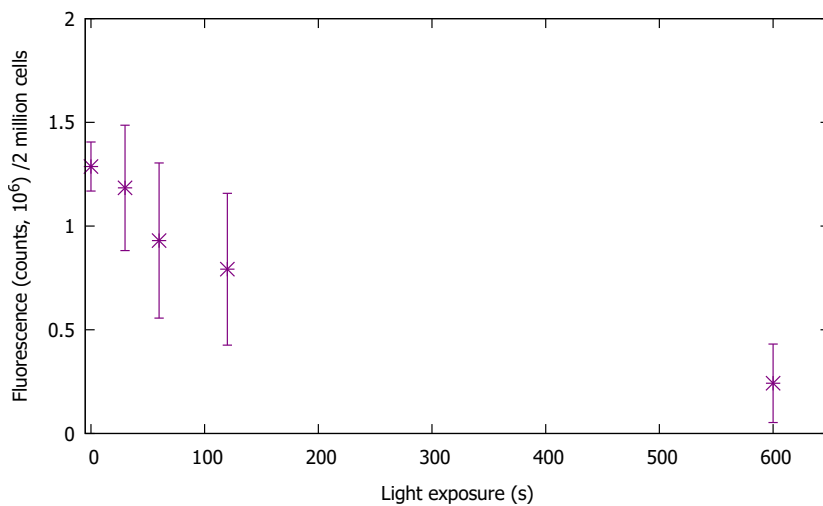


Figure 4.18: Plot of fluorescence for PpA as a function of light exposure in seconds.

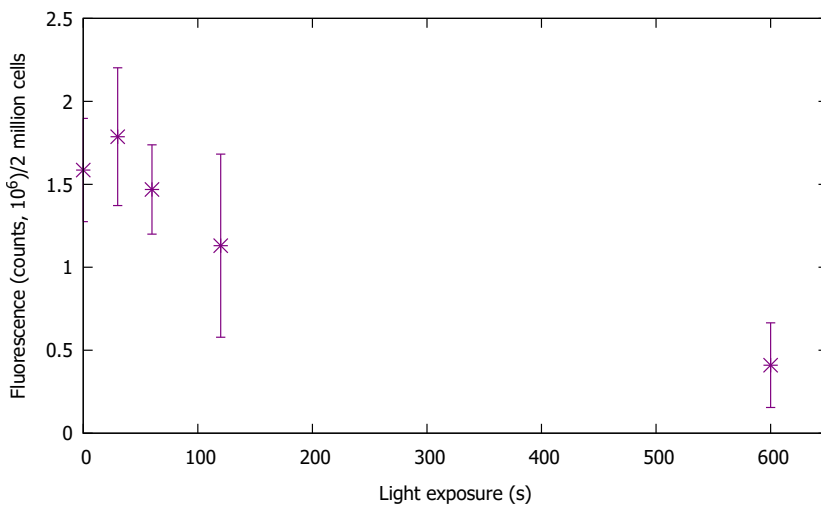


Figure 4.19: Plot of fluorescence spectrum for PpB as a function of light exposure in seconds.

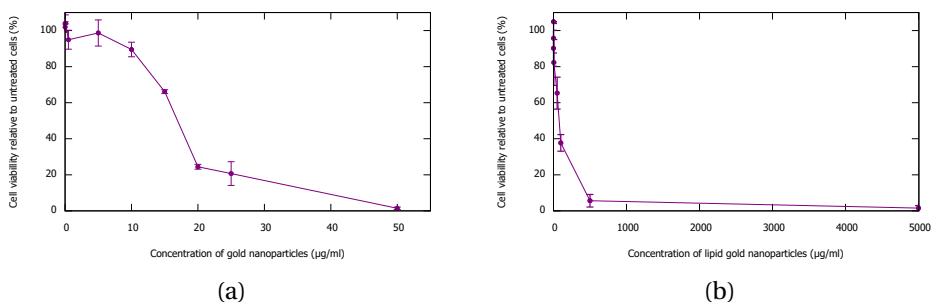


Figure 4.20: Cell viability of: (a) Gold nanoparticles at concentrations from  $0.0005 \mu\text{g/ml}$  to  $50 \mu\text{g/ml}$  in steps of power of ten. (b) gold-loaded lipid nanoparticles at concentrations from  $0.0005 \mu\text{g/ml}$  to  $5000 \mu\text{g/ml}$  in steps of power of ten.

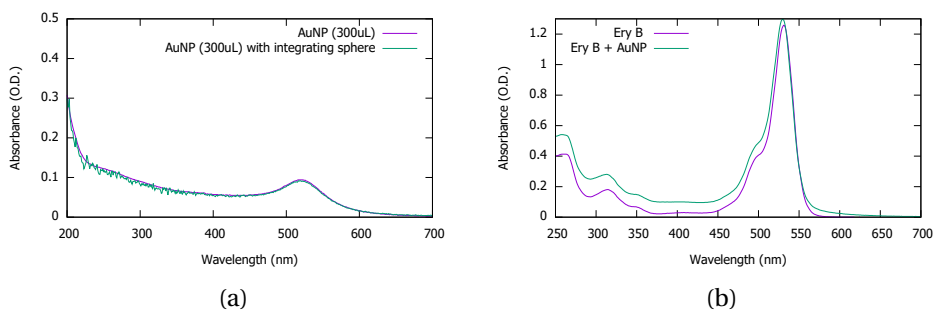


Figure 4.21: The absorption spectra of gold nanoparticles (a) and erythrosin B with added gold nanoparticles (b).

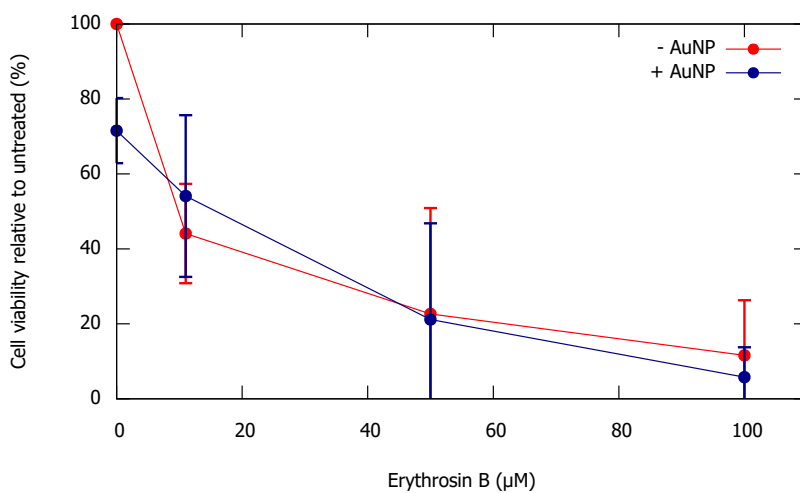


Figure 4.22: Plot of cell viability for control cells without light. With gold nanoparticles is plotted in blue and without gold nanoparticles is plotted in red.

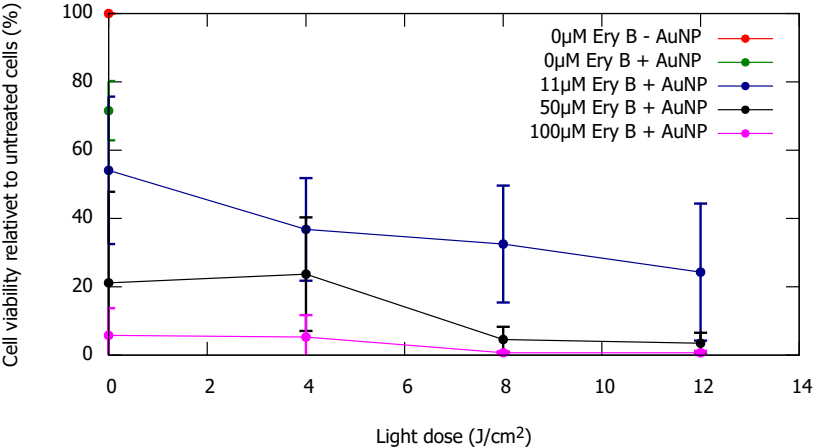


Figure 4.23: Plot of cell viability for cells with or without gold nanoparticles as a function of light exposure in seconds.



# Chapter 5

## Discussion

### 5.1 Evaluation of the protoporphyrins

#### 5.1.1 Photophysical properties

The results of the protoporphyrins PpA and PpB shows that they have very similar properties. They both have the ability of absorb at the same wavelengths, but one of the important peaks is the one at 624 nm. This is in the red light regime which is the part of the visible light that has the ability to penetrate the furthest into the skin. PpB have slightly stronger absorption as confirmed by a higher molar extinction coefficient shown in table 4.3.

Furthermore does the two protoporphyrins show similar fluorescence lifetime both being around 13.5 ns [53]. The fluorescence quantum yield of the two are close with PpA being 2% higher than PpB as shown in table 4.3. The differences between the two protoporphyrins is observed in the results of the triplet state decay and for the singlet oxygen luminescence. The triplet state absorption were used to determine which wavelengths that would used for the triplet state decay, first the smaller band at around 630 nm, but it turned out to give a signal that was too weak to measure. Then the large band at around 435 nm were used and which gave measurable results.

From the result we see that PpB shows ten times higher concentration of triplets at  $t = 0$  s than PpA, but have a lower triplet state lifetime by approximately  $30 \mu\text{s}$ . This means that PpB gets more molecules in the triplet state, but the triplet lifetime is almost 90 % of the triplet lifetime of PpA. The samples which are added air have as expected large decrease in triplet lifetime compared to the deoxygenated ones. The signal of the triplet state decay were weak and fast, making it difficult to measure. In addition was the fit of the signal poor as can be gathered from the plot of the residuals.

The lifetime of the triplet state was measured to be  $301.44 \mu\text{s}$  for PpA and  $274.86 \mu\text{s}$  for PpB. By comparing this value to the  $\tau_r$  from the singlet oxygen luminescence, they are far off. The  $\tau_r$  is  $1.93 \mu\text{s}$  for PpA and  $3.80 \mu\text{s}$ . This is to be expected as the two former are deoxygenated solutions and the two latter are with oxygen. It is a desired result as a long triplet lifetime without oxygen and short in the presence of oxygen. The values and fit of the singlet oxygen is much more reliable and therefore should be weighted more. The value of  $\tau_\Delta$  is larger for PpB than PpA, indicating a larger quenching effect of singlet oxygen for PpB, but the value of  $S_0$  of PpB is larger, making more singlet oxygen in the process.

When comparing PpA and PpB to PpIX, the absorption is a lot weaker for PpIX than for the other two. There is as mentioned previously a slight redshift of the peaks of absorption and fluorescence of PpIX compared to PpA and PpB. The fluorescence lifetime is also about 2 ns shorter for PpIX than the two other, but the fluorescence quantum yield is similar. The error, calculated using equation 3.16, is also very high for PpIX. That could mean the measurements are quite off or the calculation of uncertainty doesn't take account for some unknown parameter. This could be that the absorption values are too close to each other making the linear regression not reliable. In order get an acceptable uncertainty more measurements should be performed for PpIX. The singlet oxygen luminescence of PpIX showed both a longer  $\tau_\Delta$  and a shorter  $\tau_r$  making it more efficient in energy transfer from the triplet states and have a longer singlet oxygen lifetime. The concentration of singlet oxygen is lower for

PpIX than for the other two with  $S_0$  being 11.36 compared to 12.22 and 16.98.

In terms of PDT the choice is between efficient processes and strength of signals. The PpA have more efficient triplet transfer processes and a longer lifetime, but at the cost of lower absorption fluorescence and decisively a lower concentration of singlet oxygen. PpIX has a very low water solubility which makes it hard to administer as a medicinal drug [18]. The PpA and PpB are synthesized to have a higher water solubility and also have the same properties in PDT as the PpIX.

### 5.1.2 Photobleaching

The fluorescence photobleaching results in figures 4.16 and 4.17 indicates a trend. Both PpA and PpB are showing a decrease in fluorescence intensity at all the three peaks located at around 625 nm, 660 nm and 690 nm. When looking at the intensity of the fluorescence both the PS's they both start around 1.4 million counts in intensity with no light. Cells treated with PpA (2.5  $\mu$ M, 24 h) appears to lose intensity faster than cells treated with PpB (2.5  $\mu$ M, 24 h) for the the smaller doses. However at 1.55 J/cm<sup>2</sup>, there is a rather large drop of intensity for PpB, being close to half the intensity of PpA at same light dose. The reason for this may be the photobleaching, which is more clearly represented in figure 4.18 and 4.19. In these two figures the fluorescence maximum for different exposure times are plotted. There were in total three bleaching experiments, each point in the graphs are the mean of fluorescence maximums measured at each experiment. In figure 4.19 the datapoints at 30 seconds one observes that the fluorescence is higher than that for 0 seconds. This suggests that for PpB the light dose of 30 seconds have little effect.

There are some uncertainties regarding the numbers and measurements the data indicates a bleaching effect, though. This photobleaching is most likely to be the result of cell death caused by the photochemical reaction between protoporphyrins and the light. It is also apparent to see that PpIX (blue and red lines in figure) which is produced naturally in our

bodies, have an intensity that is very low compared to the two PS's.

## 5.2 The influence of gold nanoparticles in PDT

The three compounds perinaphthenone, eosin B and erythrosin B were all investigated and from those erythrosin B was selected to be tested with an added solution of gold nanoparticles. This addition of gold nanoparticles to the solution of erythrosin B increased not only the peak of absorption, but also the width of absorption band. The lipid gold nanoparticles were also considered, but the solution they came in were non-transparent and would be very difficult to characterize.

This promising result of the toxicity of the gold nanoparticles and the discovery of an article by Garg et al. using erythrosin B in malignant (H357) and pre-malignant (DOK) oral epithelial cells [54]. The lead to decision to try some of the same concentrations of erythrosin B and also add gold nanoparticle in AY27 cells. From figure 4.20 we can see the cell viability is high for most of the concentrations used, first at 20  $\mu\text{g}/\text{ml}$  it drops into 20%. The concentrations from 0.0005  $\mu\text{g}/\text{ml}$  to 10  $\mu\text{g}/\text{ml}$  yields from 100% to 90 % cell viability. These measurements was the reason for using a concentration of 0.005  $\mu\text{g}/\text{ml}$  gold nanoparticles.

The cells that was not exposed to light was divided into two groups, depending on if they had gold nanoparticles added to them, or not. Comparing these two, in figure 4.22, the drop in cell viability is below 60% for the cells with gold nanoparticles and 40 % for the cells without nanoparticles, which is opposite of desired. The standard deviations are rather large, but looking at the results for the higher concentrations, there is not a large difference with or without gold nanoparticles. This trend apply to all the concentrations. The reasons for the large standard standard deviation is partly due to the first experiment having much higher cell viability than the later. A possible explanation may be the stock solution of erythrosin B. Before the first cell experiment it had been stored in a refrigerator for a longer period of time, being exposed to light when

other users the refrigerator even though it was covered in aluminium. In addition was THF used as the solvent, which evaporate quite easily and could contribute to weaker effect of the stock solution, since erythrosin B may precipitate. Or it may also be a random measurement error when making the first stock solution or a random error when performing the first experiment.

As shown in figure 4.23, the cell viability of 11  $\mu\text{M}$  begins lower than expected with its mean value being below 60%, with even lower viability for 50  $\mu\text{M}$  and 100  $\mu\text{M}$ . It can be determined directly that 100  $\mu\text{M}$  is too high of a concentration to use in PDT as it has close to 5 % viability with no exposure to light. The 50  $\mu\text{M}$  has also a low viability for no light exposure, making it a concentration which is too high to use for PDT. The 11  $\mu\text{M}$  on the other hand shows a too high viability for the 12 J/cm<sup>2</sup>, but the slope of the points is going down, enabling the possibility of the use of higher light doses in a possible treatment. All of these points have to be confirmed by additional experiments and measurements for the different light doses with gold and without erythrosin B must be added as well.

## 5.3 Evaluation of singlet oxygen yielding compounds

### 5.3.1 Photophysical properties

Eosin B, erythrosin B and perinaphtenone are all compounds which are known to have a high yield of singlet oxygen. The absorption spectra are quite different, with perinaphtenone which have a broader, weaker band from 300 nm to 450 nm. This suggest absorption of UV and blue light, which is not desired in PDT as it have short penetration length. Eosin B and erythrosin B shows more promise with a band from 450 nm to 560 nm , being in the green light area. The molar extinction coefficient was almost 4 times higher for eosin B than for perinaphtenone and erythrosin

B.

The fluorescence plots in figure 4.3, shows that erythrosin B has a lot stronger fluorescence than the two other compounds as the concentration was equal for eosin B and lower than perinaphthenone. This is in accordance with existing documentation since the perinaphthenone is known for high singlet oxygen yield, this due to a large amount of the absorbed energy goes to the triplet state as seen in figure 4.8 [55].

An attempt to measure the singlet oxygen luminescence of eosin B yielded no reasonable results, which resulted in no excited state absorption measurements. The excited state absorption not showing anything could be due to the solvent that was used. The plan was to investigate other solvents, but due to time constrictions this was not carried out. Additionally a very weak fluorescence was measured for both eosin B and perinaphthenone, as stated above, making the measurements of the quantum yield difficult and the results were inconclusive. A way to improve the measurements is choosing a different excitation wavelength, try other solvents or change the reference compound. For instance has quinine sulfate a rather high quantum yield making it difficult to compare to eosin B. The weak fluorescence also made the lifetime measurements difficult. The value which was achieved for perinaphthenone was obtained after 50000 seconds in order to reach the peak of 10000 counts, making it more an approximation than an actual measurement.

Erythrosin B showed much more promise in terms of fluorescence and the fluorescence quantum yield is both quite high and the most reliable of all the measurements with a 8 % uncertainty. This further supports the argument that more points should be measured when determining the fluorescence quantum yield with absorbance values apart from each measurement point which is also recommended by Horiba [56].

The triplet state absorption showed a large signal in the region from around 570 nm to 800 nm, although the triplet decay signal was not very strong. The decay time of erythrosin B was significantly faster than perinaphthenone when the samples were deoxygenated, but when oxygen

was introduced the lifetimes were almost equal. The singlet oxygen luminescence supports the findings of the triplet state decay, with very short lifetimes, even shorter than for the protoporphyrins. Perinaphthenone has the longest singlet oxygen lifetime and higher yield than erythrosin B. In addition is the concentration of singlet oxygen higher, with over three times the value of  $S_0$  compared to erythrosin B. Interestingly the measurements of erythrosin B with and without the addition of gold nanoparticles, reveals that the gold nanoparticles quenches singlet oxygen, as the value of  $S_0$  decreases from 5.34 to 3.66. On the positive side, the gold nanoparticles did increase  $\tau_r$ , but at the same time decreased  $\tau_\Delta$ . The arguments which are in favor of gold nanoparticles is outweighed by those against. These arguments also agrees with the PDT experiments, which did not show any additional cell death comparing the cells with and without gold nanoparticles.

In terms of PDT, erythrosin B showed promising properties. This in regards of its fluorescence and the fact that it can produce singlet oxygen, although the values are quite small compared to other compounds like the protoporphyrins and perinaphthenone. Addition of gold nanoparticles did not enhance the singlet oxygen capabilities, so other approaches should be investigated.

## 5.4 Future work

Regarding the protoporphyrin measurements, a more thorough investigation of the cellular mechanisms in PDT using the compounds PpA and PpB is necessary, in order to be used in trials with living animals. These include cell viability assays like MTT and flow cytometry. The use of PpA and PpB in clinical PDT, definitely seems like an option in the future with more thorough knowledge about how they affect cells *in-vivo*.

The gold nanoparticles should be added to other compounds in order to determine if they have enhancing effect for PDT. It seemed promising with the absorption spectrum for erythrosin B and maybe other com-

pounds shows even more positive results. The negative effect they have on singlet oxygen may change with another compound or higher concentrations as the viability test showed non-toxicity for higher concentrations than used in these experiments.

Trying other modifications of erythrosin B, may give more ideal properties in terms of PDT. The solubility, singlet oxygen production, and the wavelengths for which it absorbs are among several properties that could be improved upon.

# Chapter 6

## Conclusion

A major part in this thesis has been to characterize the photophysical properties of the two protoporphyrins PpA and PpB, and compare them to PpIX. Spectroscopic techniques were used to determine their absorption, fluorescence, triplet state absorption and the ability to create singlet oxygen. The results have shown properties close to or even better than PpIX. The photobleaching effect of PpA and PpB showed a bleaching indicating PDT. When comparing the two, PpB shows more promise as it has higher fluorescence, stronger absorption and both higher singlet oxygen concentration and  $\tau_r$ . The singlet oxygen lifetime is longer for PpA, but both the two protoporphyrins show results on the same level as PpIX and can be further investigated as PS in PDT.

Eosin B, erythrosin B and perinaphthenone were all investigated as new possible PS. The absorption and especially the fluorescence of eosin B and perinaphthenone were weak compared to erythrosin B. The singlet oxygen luminescence showed that eosin B did not showed any results and though perinaphthenone showed higher concentration of singlet oxygen, rise time and singlet oxygen lifetime, the weak fluorescence lead to the investigation of erythrosin B in cells treated with light.

These light experiments also investigated effect of gold nanoparticles in PDT, by adding them to different concentrations of erythrosin B. Both singlet oxygen luminescence and MTT assays after a PDT treatment with

light showed that the gold nanoparticles did not improve the PDT effect and in fact quenched the singlet oxygen. The MTT-assays yielded that a 11  $\mu\text{M}$  molar concentration of erythrosin B had around 60% viability of no exposure to light and a slightly more than 20% for a light dose of  $12\text{ J/cm}^2$ . A lower concentration and higher lightdose may give better results.

# Bibliography

- [1] A. F. McDonagh. "Phototherapy: from ancient Egypt to the new millennium". In: *Journal of Perinatology* 21.S1 (2001), S7.
- [2] P. C. Gøtzsche. "Niels Finnsen's treatment for lupus vulgaris". In: *Journal of the Royal Society of Medicine* 104.1 (2011). PMID: 21205777, pp. 41–42. DOI: 10.1258/jrsm.2010.10k066.
- [3] Nobel Media AB. *The Nobel Prize in Physiology or Medicine 1903*. [Online; accessed 01.05.2017]  
[https://www.nobelprize.org/nobel\\_prizes/medicine/laureates/1903/](https://www.nobelprize.org/nobel_prizes/medicine/laureates/1903/). 2014.
- [4] J. D. Spikes. "The origin and meaning of the term "photodynamic" (as used in "photodynamic therapy", for example)". In: *Journal of Photochemistry and Photobiology B: Biology* 9.3 (1991), pp. 369–371. ISSN: 1011-1344. DOI: [https://doi.org/10.1016/1011-1344\(91\)80172-E](https://doi.org/10.1016/1011-1344(91)80172-E).
- [5] D. Mitton and R. Ackroyd. "A brief overview of photodynamic therapy in Europe". In: *Photodiagnosis and Photodynamic Therapy* 5.2 (2008), pp. 103–111. ISSN: 1572-1000. DOI: <https://doi.org/10.1016/j.pdpdt.2008.04.004>.
- [6] R. M. Szeimies et al. "Chapter 1 History of photodynamic therapy in dermatology". In: *Photodynamic Therapy and Fluorescence Diagnosis in Dermatology*. Ed. by P. Calzavara-Pinton, R. M. Szeimies, and B. Ortel. Vol. 2. Comprehensive Series in Photosciences. Else-

- vier, 2001, pp. 3–15. DOI: [https://doi.org/10.1016/S1568-461X\(01\)80105-8](https://doi.org/10.1016/S1568-461X(01)80105-8).
- [7] R. Ackroyd et al. “The History of Photodetection and Photodynamic Therapy”. In: *Photochemistry and Photobiology* 74.5 (2001), pp. 656–669. DOI: 10.1562/0031-8655(2001)0740656THOPAP2.0.CO2.
- [8] M. R. Hamblin and P. Mróz. “History of PDT: The First Hundred Years”. In: *Advances in Photodynamic Therapy: Basic, Translational, and Clinical*. Ed. by M. R. Hamblin and Mróz. Boston|London: Artech House, 2008. Chap. 1, pp. 1–9.
- [9] Sanderson D. R. et al. “Hematoporphyrin as a diagnostic tool. A preliminary report of new techniques”. In: *Cancer* 30.5 (1972), pp. 1368–1372. DOI: 10.1002/1097-0142(197211)30:5<1368::AID-CNCR2820300534>3.0.CO;2-H.
- [10] D. E. J. G. J. Dolmans, D. Fukumura, and R. K. Jain. “Photodynamic therapy for cancer”. In: *Nature reviews cancer* 3.5 (2003), pp. 380–387.
- [11] V. Bogoeva et al. “Ruthenium porphyrin-induced photodamage in bladder cancer cells”. In: *Photodiagnosis and photodynamic therapy* 14 (2016), pp. 9–17.
- [12] K. Konopka and T. Goslinski. “Photodynamic Therapy in Dentistry”. In: *Journal of Dental Research* 86.8 (2007). PMID: 17652195, pp. 694–707. DOI: 10.1177/154405910708600803.
- [13] P.R. Ogilby. “Singlet oxygen: there is indeed something new under the sun”. In: *Chem. Soc. Rev.* 39 (8 2010), pp. 3181–3209.
- [14] Béatrice M. Aveline. “Chapter 2 Primary processes in photosensitization mechanisms”. In: *Photodynamic Therapy and Fluorescence Diagnosis in Dermatology*. Ed. by p. Calzavara-Pinton, R. M. Szeimies, and B. Ortel. Vol. 2. Comprehensive Series in Photosciences. Elsevier, 2001, pp. 17–37. DOI: [https://doi.org/10.1016/S1568-461X\(01\)80106-X](https://doi.org/10.1016/S1568-461X(01)80106-X).

- [15] M. Ethirajan et al. "Photosensitizers for Photodynamic Therapy and Imaging". In: *Advances in Photodynamic Therapy: Basic, Translational, and Clinical*. Ed. by M. R. Hamblin and Mróz. Boston|London: Artech House, 2008. Chap. 2, pp. 13–37.
- [16] PubChem. *Porphyrin and Heme Metabolism*. [Online; accessed 21.12.2017] <https://themedicalbiochemistrypage.org/heme-porphyrin.php>. 2017.
- [17] Epomedicine. *Heme synthesis pathway*. [Online; accessed 31.05.2018] [urlhttp://epomedicine.com/wp-content/uploads/2016/07/heme-synthesis-pathway.jpg](http://epomedicine.com/wp-content/uploads/2016/07/heme-synthesis-pathway.jpg). 2018.
- [18] PubChem. *Protoporphyrin IX*. [Online; accessed 18.12.2017] <https://pubchem.ncbi.nlm.nih.gov/image/imagefly.cgi?cid=4971&width=500&height=500>. 2017.
- [19] Q. Peng et al. "5-Aminolevulinic acid-based photodynamic therapy". In: *Cancer* 79.12 (1997), pp. 2282–2308.
- [20] E. Glimsdal. "Spectroscopic characterization of some platinum acetylide molecules for optical power limiting applications". PhD thesis. Trondheim, Norway: NTNU – Norges teknisk-naturvitenskapelige universitet, 2009.
- [21] S. N. Næss et al. "Molecular biophysics". Compendium. 2017.
- [22] A. Hauge. "Amphinex-(TPCS<sub>2a</sub>)-based photodynamic therapy and photochemical internalization of bleomycin and temozolomide- in vitro studies on the glioma cell line F98". MA thesis. Trondheim, Norway: NTNU – Norges teknisk-naturvitenskapelige universitet, 2013.
- [23] D. J. Griffiths. *Introduction to quantum mechanics*. Pearson, 2014.
- [24] M. K. Siksjø. "Biophysical Studies of Light Sensistive Chromophores in Rat Glioma and Chinese Hamster Ovary Cancer cells". MA thesis. Trondheim, Norway: NTNU – Norges teknisk-naturvitenskapelige universitet, 2015.

- [25] D. J. Griffiths. *Principles of Fluorescence Spectroscopy*. Kluwer Academic/Plenum Publishers, 1999.
- [26] J. W. Lichtman and J.-A. Conchello. “Fluorescence microscopy”. In: *Nature methods* 2.12 (2005), p. 910.
- [27] R. Bonnett and G. Martinez. “Photobleaching of sensitisers used in photodynamic therapy”. In: *Tetrahedron* 57.47 (2001), pp. 9513–9547.
- [28] O. A. Gederaas et al. “Photochemical internalization in bladder cancer - development of an orthotopic in vivo model.” In: *J. Photochem Photobiol Sci.* 16 (2017), pp. 1664–1676.
- [29] T. Mosmann. “Rapid colorimetric assay for cellular growth and survival: Application to proliferation and cytotoxicity assays”. In: *Journal of Immunological Methods* 65.1 (1983), pp. 55–63. ISSN: 0022-1759. DOI: [https://doi.org/10.1016/0022-1759\(83\)90303-4](https://doi.org/10.1016/0022-1759(83)90303-4).
- [30] N. C. Thomas. “The early history of spectroscopy”. In: *Journal of chemical education* 68.8 (1991), p. 631.
- [31] D. J. S. Hungerford G. and Birch. “Single-photon timing detectors for fluorescence lifetime spectroscopy”. In: *Measurement Science and Technology* 7.2 (1996), p. 121.
- [32] G. Porter. “Flash photolysis and spectroscopy. A new method for the study of free radical reactions”. In: *Proc. R. Soc. Lond. A* 200.1061 (1950), pp. 284–300.
- [33] J. W. Snyder et al. “Optical detection of singlet oxygen from single cells”. In: *Physical Chemistry Chemical Physics* 8.37 (2006), pp. 4280–4293.
- [34] O. A. Gederaas. “Biological mechanisms involved in 5-aminolevulinic acid based photodynamic therapy”. PhD thesis. Trondheim, Norway: NTNU – Norges teknisk-naturvitenskapelige universitet, 2000.

- [35] Harvard.edu. *A Summary of Error Propagation*. [Online; accessed 29.05.2018]  
[http://ipl.physics.harvard.edu/wp-uploads/2013/03/PS3\\$\\_Error\\$\\_Propagation\\$\\_\\$sp13.pdf](http://ipl.physics.harvard.edu/wp-uploads/2013/03/PS3$_Error$_Propagation$_$sp13.pdf).
- [36] Gordon Leslie Squires. *Practical physics*. Cambridge university press, 2001.
- [37] Hitachi. *3010/3310*. [Online; accessed 31.05.2018]  
<http://www.labequip.com/stock/pictures/30389.pdf>.
- [38] Mettler Toledo. *Operating instructions*. [Online; accessed 31.05.2018]  
<http://www.americaninstrument.com/pdf/0665C-BALANCE.pdf>].
- [39] Sigma Aldrich. *Transferpette® Testing Instructions (SOP)*. [Online; accessed 01.06.2018]  
<https://www.sigmaaldrich.com/technical-documents/articles/biology/brand/transferpette-testing-instructions-sop.html>.
- [40] Thermo scientific. *Thermo Scientific Finnpiptette Performance Specifications*. [Online; accessed 01.06.2018]  
<https://static.thermoscientific.com/images/D20949~.pdf>.
- [41] T. Williams, C. Kelley, and many others. *Gnuplot 5.2: an interactive plotting program*. <http://gnuplot.sourceforge.net/>. May 2018.
- [42] R. M. Ion et al. "The incorporation of various porphyrins into blood cells measured via flow cytometry, absorption and emission spectroscopy". In: *ACTA BIOCHIMICA POLONICA-ENGLISH EDITION*-45 (1998), pp. 833–845.
- [43] M. Gouterman. "Spectra of porphyrins". In: *Journal of Molecular Spectroscopy* 6 (1961), pp. 138–163. ISSN: 0022-2852. DOI: [https://doi.org/10.1016/0022-2852\(61\)90236-3](https://doi.org/10.1016/0022-2852(61)90236-3).

- [44] A. M Brouwer. “Standards for photoluminescence quantum yield measurements in solution (IUPAC Technical Report)”. In: *Pure and Applied Chemistry* 83.12 (2011), pp. 2213–2228.
- [45] Laurent Porres et al. “Absolute measurements of photoluminescence quantum yields of solutions using an integrating sphere”. In: *Journal of fluorescence* 16.2 (2006), pp. 267–273.
- [46] E. M. García et al. “Methods for analysis of time-resolved fluorescence data”. In: *CONIELECOMP 2012, 22nd International Conference on Electrical Communications and Computers*. Feb. 2012, pp. 317–322. DOI: 10.1109/CONIELECOMP.2012.6189931.
- [47] R. Bonnett et al. “PHOTOPHYSICAL PROPERTIES OF meso-TETRAPHENYLPORP and SOME meso-TETRA (HYDROXYPHENYL) PORPHYRINS”. In: *Photochemistry and photobiology* 48.3 (1988), pp. 271–276.
- [48] B. Giner et al. “Study of Weak Molecular Interactions through Thermodynamic Mixing Properties”. In: *The Journal of Physical Chemistry B* 110.35 (2006). PMID: 16942115, pp. 17683–17690. DOI: 10.1021/jp062583q.
- [49] Chemical Book. *Sulfuric acid*. [Online; accessed 01.06.2018] [https://www.chemicalbook.com/ProductMSDSDetailCB9675634\\_EN.htm](https://www.chemicalbook.com/ProductMSDSDetailCB9675634_EN.htm).
- [50] S. Kedenburg et al. “Linear refractive index and absorption measurements of nonlinear optical liquids in the visible and near-infrared spectral region”. In: *Optical Materials Express* 2.11 (2012), pp. 1588–1611.
- [51] Chemical Book. *Sodium hydroxide*. [Online; accessed 01.06.2018] [http://www.chemicalbook.com/ChemicalProductProperty\\_EN\\_CB8105015.htm](http://www.chemicalbook.com/ChemicalProductProperty_EN_CB8105015.htm).
- [52] S. Eustis and M. A. El-Sayed. “Why gold nanoparticles are more precious than pretty gold: noble metal surface plasmon resonance and its enhancement of the radiative and nonradiative properties

- of nanocrystals of different shapes". In: *Chemical society reviews* 35.3 (2006), pp. 209–217.
- [53] B. Minaev and M. Lindgren. "Vibration and fluorescence spectra of porphyrin-cored bis (methylo)-propionic acid dendrimers". In: *Sensors* 9.3 (2009), pp. 1937–1966.
- [54] A. D. Garg et al. "In vitro studies on erythrosine-based photodynamic therapy of malignant and pre-malignant oral epithelial cells". In: *PLoS One* 7.4 (2012), e34475.
- [55] R. Schmidt et al. "Phenalenone, a universal reference compound for the determination of quantum yields of singlet oxygen O<sub>2</sub> (<sup>1</sup>Δ<sub>g</sub>) sensitization". In: *Journal of Photochemistry and Photobiology A: Chemistry* 79.1-2 (1994), pp. 11–17.
- [56] Horiba UK limited. *A guide to recording fluorescence quantum yields*. [Online; accessed 05.06.2018]  
<http://www.horiba.com/fileadmin/uploads/Scientific/Documents/Fluorescence/quantumyieldstrad.pdf>.



# **Appendix A**

## **Additional plots and results**

### **A.1 Triplet state decay**

### **A.2 Singlet Oxygen**

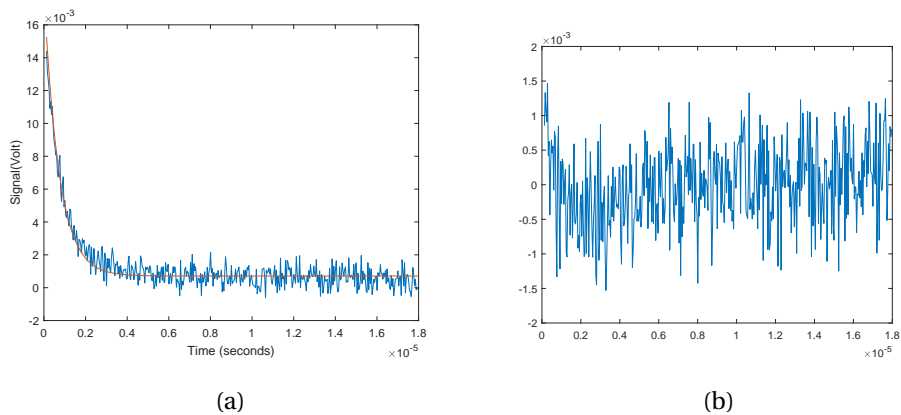


Figure A.1: Plot of the: (a) Triplet state decay of erythrosin B measured at 650 nm (b) the residual of the fit (b)

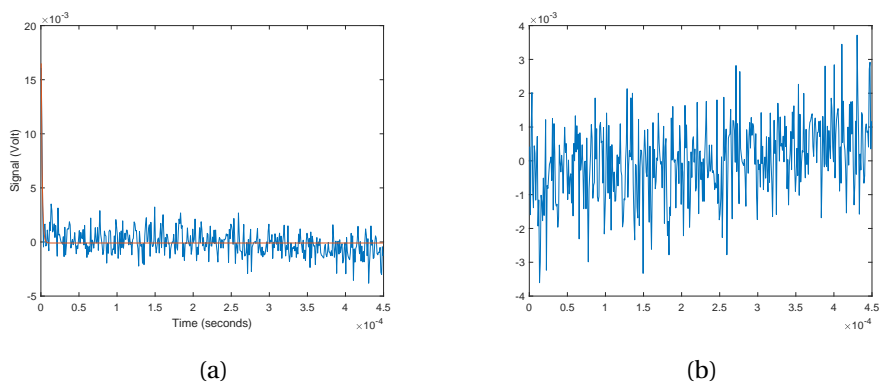


Figure A.2: Plot of the: (a) Triplet state decay of PpA measured at 435 nm with air (b) and the residual of the fit (b)

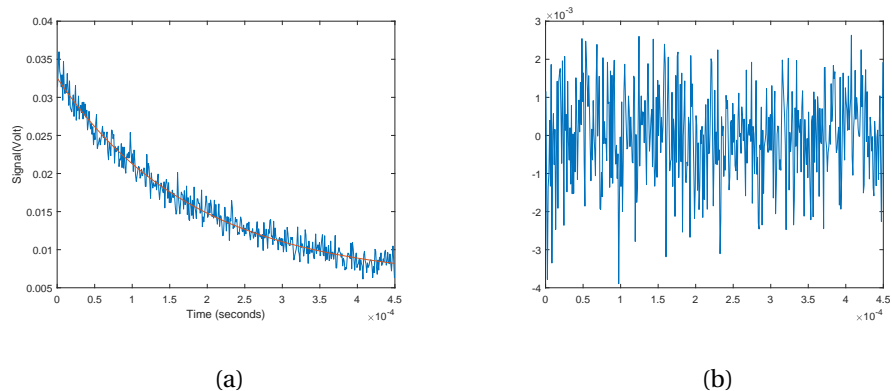


Figure A.3: Plot of the: (a) Triplet state decay of PpB measured at 435 nm with air (b) and the residual of the fit (b)

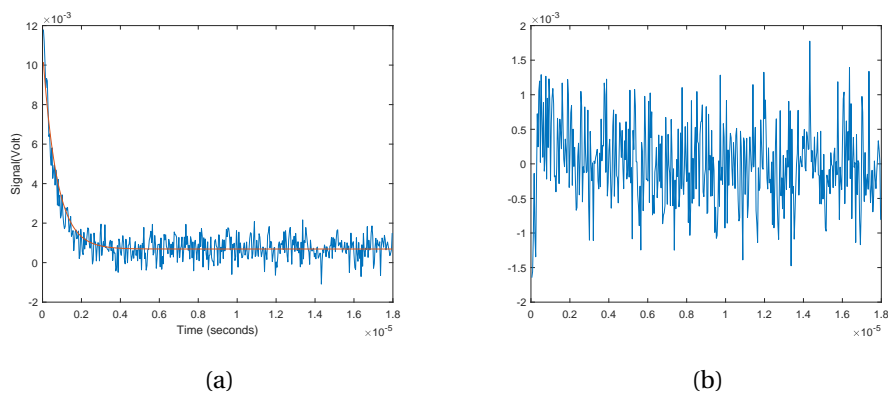
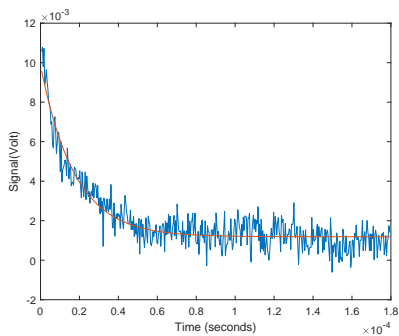
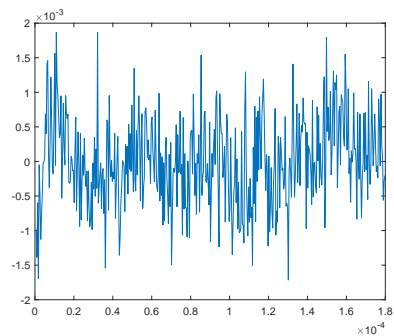


Figure A.4: Plot of the: (a) Triplet state decay of perinaphthenone measured at 460 nm with air (b) The residual of the fit

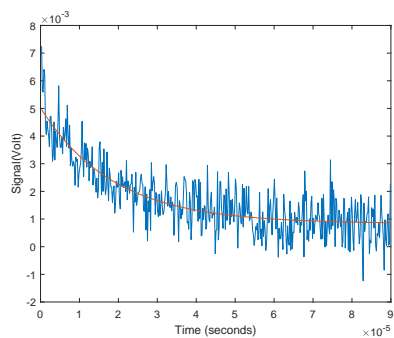


(a) Triplet decay

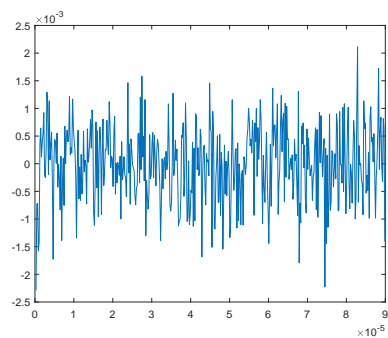


(b) Residuals of fit

Figure A.5: Plot of the: (a) Triplet state decay of perinaphthenone measured at 460 nm (b) The residual of the fit



(a) Triplet decay



(b) Residuals of fit

Figure A.6: Plot of the: (a) Triplet state decay of PpIX measured at 660 nm (b) The residual of the fit

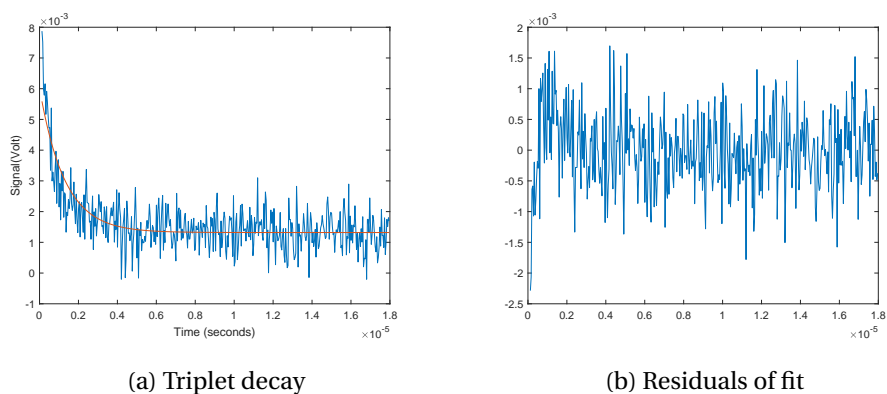


Figure A.7: Plot of the: (a) Triplet state decay of perinaphthenone measured at 660 nm with air (b) The residual of the fit

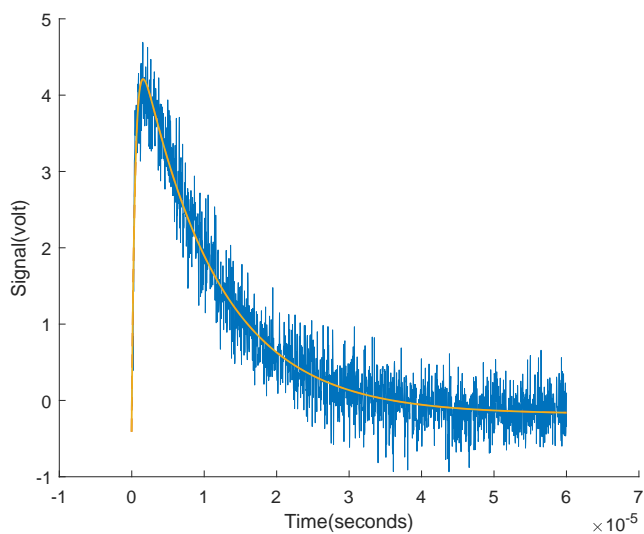


Figure A.8: Plot of singlet oxygen luminiscence from erythrosin B. Analyzed by Matlab and fitted to determine the rise time and lifetime.

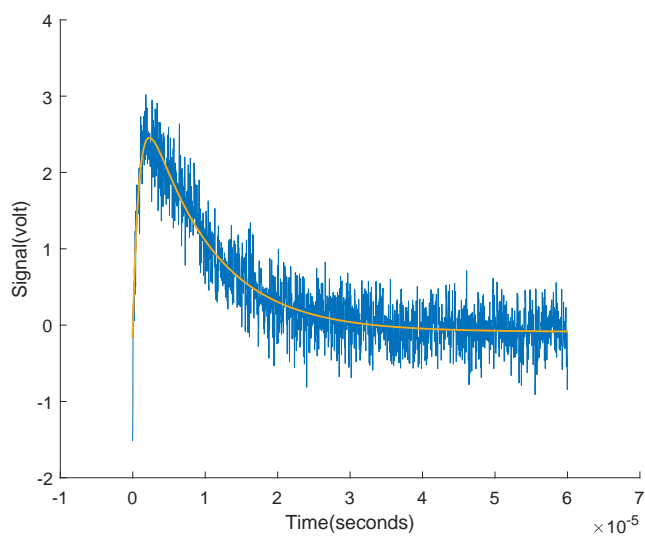


Figure A.9: Plot of singlet oxygen luminiscence from erythrosin B with gold nanoparticles. Analyzed by Matlab and fitted to determine the rise time and lifetime.

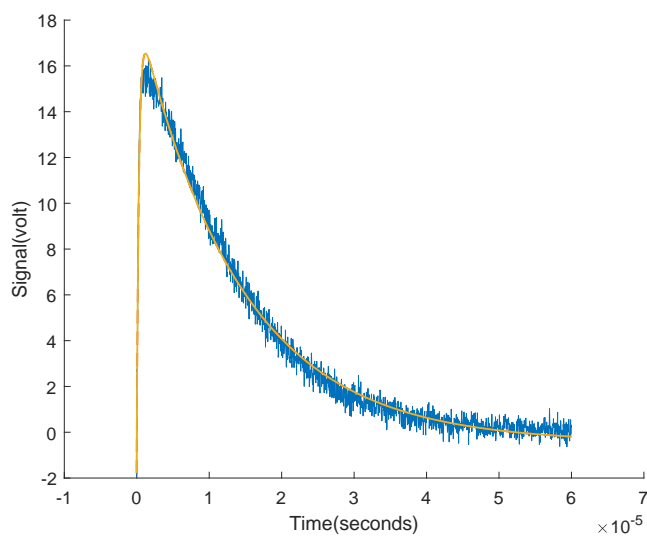


Figure A.10: Plot of singlet oxygen luminiscence from Perinaphthenone. Analyzed by Matlab and fitted to determine the rise time and lifetime.



## **Appendix B**

### **PCI Biotech LumiSource**

### 3 Technical information LumiSource®

#### 3.1 Description and components

The LumiSource® is designed specifically to provide homogeneous illumination of living cells in an invitro setting. The lamp consists of light tubes with reflectors designed to provide stable, homogeneous fluency rate over a defined illumination area of 45 x 17 cm. In addition to the tubes, the lamp consists of a removable top plate and a shutter.

The LumiSource® is delivered with a bank of 4 light tubes (4 x 18W Osram L 18/67, Blue) emitting mainly blue light with a peak wavelength of approximately 435 nm.

These light tubes are intended for use in the PCI technology together with the photosensitiser LumiTrans® (supplied by PCI Biotech). The light emission from LumiSource® is selected for optimal excitation of LumiTrans®. (Fig. 1)

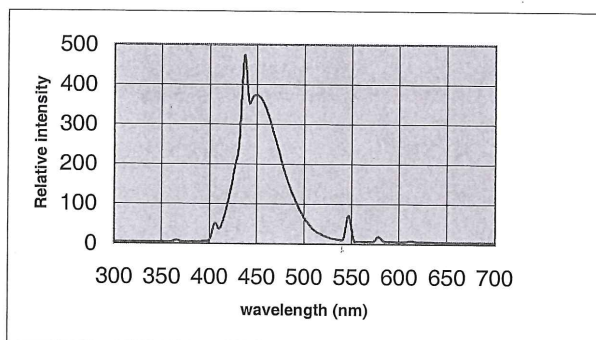


Fig.1 Spectra from standard light tubes (4 x 18W Osram L 18/67, Blue)

#### 3.2 Light emission

It is of great importance that the light emission is stable over the whole illumination area and that the intensity remains stable over time. The variation in light intensity should be minimised in order to get comparable results from experiment to experiment.

The light intensity of LumiSource® varies less than 10% across the illumination area, except for 1 cm from the corners in each direction where the intensity is 15% lower (see Fig. 2-3)

The light emission of the lamp has been measured as indicated in Fig. 2 showing the homogeneity over the light field. The irradiance of the illumination area in the middle of the field is ca. 13.5 mW /cm<sup>2</sup> (measured by IL 1700 Research Radiometer from International Light).

Note that each lamp will be delivered with information about exact irradiance.

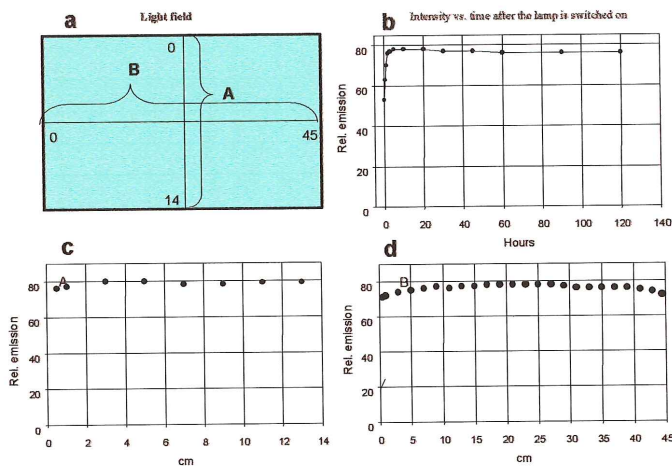


**Fig 2. Measurements of relative light emission from the illumination area of LumiSource®.** a) shows the illumination area and how light emission has been measured in figure c) and d). The light field in LumiSource® is 14 x 45 cm and the measurements shown in c) and d) were performed as indicated in a). In b) light emission has been measured at different time intervals after the lamp has been switched on. The light emission is stable for at least 24 h after the lamp has been switched on.

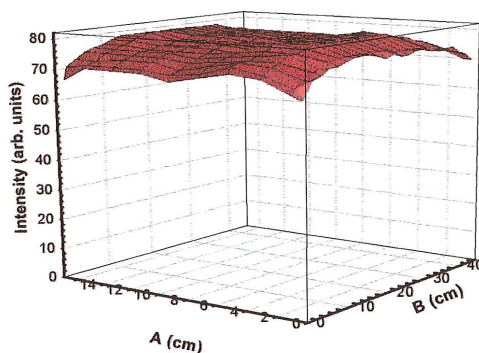


**Fig.3. 3D-profile of the light intensity emitted from LumiSource® with A and B as in Fig.2.**

### 3.3 Change of light tubes and filters

If sensitizers that are excited at other wavelengths than around 4-500 nm are used, the standard light tubes can easily be removed and replaced with new tubes.

#### Removal/change of tubes

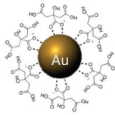
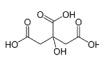
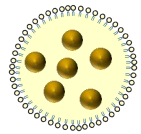
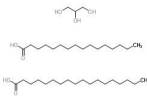
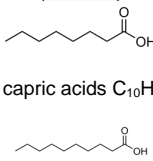
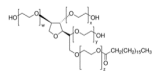
Turn off the power and remove the power plug from the socket. Remove the top plate, pull out the shutter, and remove the end reflectors by carefully pulling upwards. Then remove the tubes. Insert new tubes. Place the reflectors and the top plate back and close the shutter. Note that you can only use 18 W light tubes!

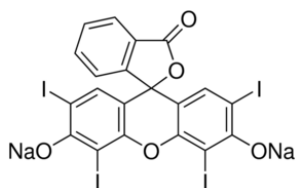


# **Appendix C**

## **Structural information**

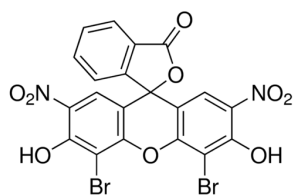
Below is the structural information about the gold nanoparticles, the lipid gold nanoparticles, eosin B, erythrosin B and perinaphthenone.

Nanoparticles	Composition	Concentration (mg/ml)	Suspension solution	Size (nm)	Zeta potential (mV)
Gold nanoparticles 	Capping agent: Citrate (C <sub>6</sub> H <sub>8</sub> O <sub>7</sub> ) 	0.05	Citrate buffer (2mM)	25	-21
	Gold				
Gold-loaded lipid nanoparticles 	<b>Solid lipid:</b> Glyceryl palmitostearate (C <sub>37</sub> H <sub>76</sub> O <sub>7</sub> ) 	56.8 (lipid mass) 0.05 (gold NPs)	Ultrapure water	215	-37
	<b>Liquid lipid:</b> Mygliol 812 (caprylic (C <sub>8</sub> H <sub>16</sub> O <sub>2</sub> ) and capric acids C <sub>10</sub> H <sub>20</sub> O <sub>2</sub> ) 				
	<b>Surfactant:</b> Polyethylene glycol sorbitan monostearate (C <sub>64</sub> H <sub>126</sub> O <sub>26</sub> ) 				
	Gold nanoparticles				

**Erythrosin B**

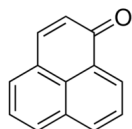
Molecular Formula:  $C_{20}H_6I_4Na_2O_5H_2O$

Molecular Weight: 835.897 g/mol

**Eosin B**

Molecular Formula:  $C_{20}H_8Br_2N_2O_9$

Molecular Weight: 580.09 g/mol

**Perinaphthenone**

Molecular Formula:  $C_{13}H_8O$

Molecular Weight: 180.20 g/mol